

Riemannian block SPD coupling manifold and its application to optimal transport

Andi Han* Bamdev Mishra[†] Pratik Jawanpuria[†] Junbin Gao*

Abstract

Optimal transport (OT) has seen its popularity in various fields of applications. We start by observing that the OT problem can be viewed as an instance of a general symmetric positive definite (SPD) matrix-valued OT problem, where the cost, the marginals, and the coupling are represented as block matrices and each component block is a SPD matrix. The summation of row blocks and column blocks in the coupling matrix are constrained by the given block-SPD marginals. We endow the set of such block-coupling matrices with a novel Riemannian manifold structure. This allows to exploit the versatile Riemannian optimization framework to solve generic SPD matrix-valued OT problems. We illustrate the usefulness of the proposed approach in several applications.

1 Introduction

Optimal transport offers a systematic approach to compare probability distributions by finding a transport plan (coupling) that minimizes the cost of transporting mass from one distribution to another. Optimal transport has been successfully applied in a wide range of fields, such as computer graphics [SDGP⁺15, SRGB14], graph representation learning [CGC⁺20, PMEGCF19], text classification [YCC⁺19], and domain adaptation [CFTR16, CFT14], to name a few.

Despite the popularity of OT, existing OT formulations are mostly limited to transporting scalar-valued mass. Applications such as diffusion tensor imaging [LBMP⁺01], image set classification [HWS⁺15, HSH14], anisotropic diffusion [Wei98], involve symmetric positive definite (SPD) matrix-valued distributions. In brain imaging particularly, where the local diffusion of water molecules are encoded in a SPD matrix [AP08], being able to compare fields of such SPD matrices is crucial. This, however, requires a nontrivial generalization of existing optimal transport framework with careful construction of cost and transport plan.

In the quantum mechanics setting, existing works [JNG12, CM14, CGT17, CGT18] have explored geodesic formulation of the Wasserstein distance between vector and matrix-valued densities. In [Nin13, NGT14], the Monge-Kantorovich optimal mass transport problem has been studied for comparing matrix-valued power spectra measures. Recently, [PCVS19] proposed to solve an unbalanced optimal transport problem for SPD-valued distributions of unequal masses.

In this paper, we propose a general framework for solving the balanced OT problem between SPD-valued distributions, where the cost and the coupling are represented as block SPD matrices. We discuss a Riemannian manifold structure for the set of such block coupling matrices that allows

*Discipline of Business Analytics, University of Sydney. Email: {andi.han, junbin.gao}@sydney.edu.au.

[†]Microsoft India. Email: {bamdevm, pratik.jawanpuria}@microsoft.com.

to use the Riemannian optimization framework [AMS08, Bou20] to solve various generalized OT problems. Specifically, our contributions are the following.

1. We introduce the general SPD matrix-valued balanced OT problem for block SPD marginals. We study the metric properties of the proposed formulation and discuss its relationship with the 2-Wasserstein distance.
2. We propose a novel manifold structure for the set of block SPD coupling matrices, which generalizes the manifold structures studied in [DH19, SGH⁺21, MSDKJ21, MKJ19]. We discuss optimization-related ingredients like Riemannian metric, Riemannian gradient, Hessian, and retraction.
3. We extend our SPD-valued balanced OT formulation to block SPD Wasserstein barycenter and Gromov-Wasserstein OT.
4. We empirically illustrate the benefit of the proposed framework in domain adaptation, tensor-valued shape interpolation, and displacement interpolation between tensor fields.

Organizations. We start with a brief review of optimal transport and Riemannian optimization in Section 2. In Section 3, we introduce the generalized SPD matrix-valued OT problem. Section 4 derives the necessary Riemannian optimization ingredients. Section 5 develops two extensions to the matrix-valued OT problem. In Section 6, we test the proposed framework in various applications. In the appendix sections, we provide the proofs and show additional experiments.

2 Preliminaries

2.1 Optimal transport

Consider two discrete measures supported on \mathbb{R}^d , $\mu = \sum_{i=1}^m p_i \delta_{\mathbf{x}_i}$, $\nu = \sum_{j=1}^n q_j \delta_{\mathbf{y}_j}$, where $\mathbf{x}_i, \mathbf{y}_j \in \mathbb{R}^d$. The weights $\mathbf{p} \in \Sigma_m, \mathbf{q} \in \Sigma_n$ are in probability simplex, i.e., $\sum_i p_i = \sum_j q_j = 1$, for $p_i, q_j \geq 0$ and $\delta_{\mathbf{x}}$ is the Dirac at \mathbf{x} . The 2-Wasserstein distance between μ, ν is given by solving the Monge-Kantorovich optimal transport problem:

$$W_2^2(\mathbf{p}, \mathbf{q}) = \min_{\gamma \in \Pi(\mathbf{p}, \mathbf{q})} \sum_{i,j} \|\mathbf{x}_i - \mathbf{y}_j\|^2 \gamma_{i,j}, \quad (1)$$

where $\Pi(\mathbf{p}, \mathbf{q}) := \{\gamma \in \mathbb{R}^{m \times n} : \gamma \geq 0, \gamma \mathbf{1} = \mathbf{p}, \gamma^\top \mathbf{1} = \mathbf{q}\}$ is the space of joint distribution between the source and the target marginals. An optimal solution of (1) is referred to as an optimal transport plan (or coupling). Recently, [Cut13] proposed the Sinkhorn-Knopp algorithm [Sin64, Kni08] for entropy-regularized OT formulation. For a recent survey of OT literature and related machine learning applications, please refer to [PC⁺19].

2.2 Riemannian optimization

A matrix manifold \mathcal{M} is a smooth subset of the ambient vector space \mathcal{V} with local bijectivity to the Euclidean space. A Riemannian manifold is a manifold endowed with a Riemannian metric (a smooth, symmetric positive definite inner product structure $\langle \cdot, \cdot \rangle_x$) on every tangent space $T_x \mathcal{M}$. The induced norm on the tangent space is thus $\|u\|_x = \sqrt{\langle u, u \rangle_x}$.

The orthogonal projection operation for an embedded matrix manifold $P_x : \mathcal{V} \rightarrow T_x\mathcal{M}$ is a projection that is orthogonal with respect to the Riemannian metric $\langle \cdot, \cdot \rangle_x$. Retraction is a smooth map from tangent space to the manifold. That is, for any $x \in \mathcal{M}$, retraction $R_x : T_x\mathcal{M} \rightarrow \mathcal{M}$ such that 1) $R_x(0) = x$ and 2) $DR_x(0)[u] = u$, where $Df(x)[u]$ is the derivative of a function at x along direction u .

The Riemannian gradient of a function $F : \mathcal{M} \rightarrow \mathbb{R}$ at x , denoted as $\text{grad}F(x)$ generalizes the notion of the Euclidean gradient, which is defined as the unique tangent vector satisfying $\langle \text{grad}F(x), u \rangle_x = DF(x)[u] = \langle \nabla F(x), u \rangle_2$ for any $u \in T_x\mathcal{M}$. $\nabla F(x)$ is the Euclidean gradient and $\langle \cdot, \cdot \rangle_2$ denotes the Euclidean inner product. To minimize the function, Riemannian gradient descent [AMS08] and other first-order solvers apply retraction to update the iterates along the direction of negative Riemannian gradient while staying on the manifold, i.e., $x_{t+1} = R_{x_t}(-\eta \text{grad}F(x_t))$, where η is the step size. Similarly, the Riemannian Hessian $\text{Hess}F(x) : T_x\mathcal{M} \rightarrow T_x\mathcal{M}$ is defined as the covariant derivative of Riemannian gradient. Popular second-order methods, such as trust regions and cubic regularized Newton's methods have been adapted to Riemannian optimization [ABG07, ABBC18].

3 Block SPD optimal transport

Consider the same setting as in Section 2.1, with two given measures $\mu = \sum_{i=1}^m p_i \delta_{\mathbf{x}_i}$, $\nu = \sum_{j=1}^n q_j \delta_{\mathbf{y}_j}$ and the marginals $\mathbf{p} \in \Sigma_m$ and $\mathbf{q} \in \Sigma_n$.

We consider *lifting* the given probability measures to a space of matrix-valued measures where an associated *mass* is represented as a positive semi-definite matrix. To this end, we convert the marginals \mathbf{p} and \mathbf{q} to block matrices \mathbf{P} and \mathbf{Q} , where $\mathbf{P} := \{[\mathbf{P}_i]_{m \times 1} : \mathbf{P}_i = p_i \mathbf{I}\}$ and $\mathbf{Q} := \{[\mathbf{Q}_j]_{n \times 1} : \mathbf{Q}_j = q_j \mathbf{I}\}$. Here, $[\cdot]_{m \times n}$ denotes a collection of mn matrices organized as a block matrix and \mathbf{I} represents the identity matrix. The cost of transporting a positive semi-definite (matrix) mass \mathbf{A} from position \mathbf{x}_i to \mathbf{y}_j is parameterized by a (given) positive semi-definite matrix $\mathbf{C}_{i,j}$ and is computed as $\text{tr}(\mathbf{C}_{i,j} \mathbf{A})$. Under this setting, we propose a block SPD matrix valued OT problem as

$$\text{MW}^2(\mathbf{P}, \mathbf{Q}) := \min_{\mathbf{\Gamma} \in \Pi(m, n, d, \mathbf{P}, \mathbf{Q})} \sum_{i,j} \text{tr}(\mathbf{C}_{i,j} \mathbf{\Gamma}_{i,j}), \quad (2)$$

where $\mathbf{\Gamma} = [\mathbf{\Gamma}_{i,j}]_{m \times n}$ is a block-matrix coupling of size $m \times n$ and the set of such couplings are defined as $\Pi(m, n, d, \mathbf{P}, \mathbf{Q}) := \{[\mathbf{\Gamma}_{i,j}]_{m \times n} : \mathbf{\Gamma}_{i,j} \in \mathbb{S}_+^d, \sum_j \mathbf{\Gamma}_{i,j} = \mathbf{P}_i, \sum_i \mathbf{\Gamma}_{i,j} = \mathbf{Q}_j, \forall i \in [m], j \in [n]\}$. Here \mathbb{S}_+^d is used to denote the set of $d \times d$ positive semi-definite matrices and $\text{tr}(\cdot)$ is the matrix trace. With a slight abuse of notation, let $\text{MW}(\mathbf{p}, \mathbf{q}) := \text{MW}(\mathbf{P}, \mathbf{Q})$ with \mathbf{P}, \mathbf{Q} defined above. Below we compare the generalized distance $\text{MW}(\mathbf{p}, \mathbf{q})$ to $W_2(\mathbf{p}, \mathbf{q})$ and analyze its metric properties.

Relationship with $W_2(\mathbf{p}, \mathbf{q})$. The 2-Wasserstein distance $W_2(\mathbf{p}, \mathbf{q})$ considers the transportation cost of a unit mass from \mathbf{x}_i to \mathbf{y}_j as $\|\mathbf{x}_i - \mathbf{y}_j\|^2$, which can be rewritten as $\text{tr}((\mathbf{x}_i - \mathbf{y}_j)(\mathbf{x}_i - \mathbf{y}_j)^\top)$. Hence, if we consider the cost for the proposed OT problem (2) as $\mathbf{C}_{i,j} = (\mathbf{x}_i - \mathbf{y}_j)(\mathbf{x}_i - \mathbf{y}_j)^\top$, then $\text{MW}(\mathbf{p}, \mathbf{q}) = W_2(\mathbf{p}, \mathbf{q})$ where the optimal block-matrix coupling is $\mathbf{\Gamma}^* = \boldsymbol{\gamma}^* \otimes \mathbf{I}$ where $\boldsymbol{\gamma}^*$ is the optimal coupling for $W_2(\mathbf{p}, \mathbf{q})$ and \otimes is the Kronecker product.

Metric properties of $\text{MW}(\mathbf{p}, \mathbf{q})$. In the following proposition, we formalize the conditions under which $\text{MW}(\mathbf{p}, \mathbf{q})$ is a valid distance metric.

Proposition 3.1. *Suppose the marginals $\mathbf{p}, \mathbf{q} \in \Sigma_n$ have the same support and the costs $\{\mathbf{C}_{i,j}\}_{i,j=1}^n$ satisfy*

1. $\mathbf{C}_{i,j} = \mathbf{C}_{j,i}$ and
2. $\mathbf{C}_{i,j} \succ \mathbf{0}$ for $i \neq j$ and $\mathbf{C}_{i,j} = \mathbf{0}$ for $i = j$,
3. $\forall (i, j, k) \in [n]^3$, and $\mathbf{A} \succeq \mathbf{0}$, $\sqrt{\text{tr}(\mathbf{C}_{i,j}\mathbf{A})} \leq \sqrt{\text{tr}(\mathbf{C}_{i,k}\mathbf{A})} + \sqrt{\text{tr}(\mathbf{C}_{j,k}\mathbf{A})}$.

Then, $\text{MW}(\mathbf{p}, \mathbf{q})$ is a metric between the marginals \mathbf{p} and \mathbf{q} .

We remark that the conditions on $\mathbf{C}_{i,j}$ in Proposition 3.1 generalize the conditions required for $\text{W}_2(\mathbf{p}, \mathbf{q})$ in (1) to be a metric. See for example [PC⁺19, Proposition 2.2]. In Appendix B, we discuss some particular constructions of the cost that satisfy the conditions.

The previous discussion on $\text{MW}(\mathbf{p}, \mathbf{q})$ motivates the generalized SPD matrix valued OT problem (2) where the marginals are arbitrary positive semi-definite matrix mass. That is, $\mathbf{P} := \{[\mathbf{P}_i]_{m \times 1} : \mathbf{P}_i \in \mathbb{S}_+^d\}$ and $\mathbf{Q} := \{[\mathbf{Q}_j]_{n \times 1} : \mathbf{Q}_j \in \mathbb{S}_+^d\}$ and \mathbf{P} and \mathbf{Q} have the same total mass. Without loss of generality, we assume $\sum_i \mathbf{P}_i = \sum_j \mathbf{Q}_j = \mathbf{I}$. The problem is well-defined provided that the corresponding coupling constraint set $\Pi(m, n, d, \mathbf{P}, \mathbf{Q})$ is non-empty. This is discussed in Section 4.

In the next section, we analyze the coupling constraint set $\Pi(m, n, d, \mathbf{P}, \mathbf{Q})$ and show that it can be endowed with a manifold structure. This allows to exploit the versatile Riemannian optimization framework to solve (2) and any more general problem [AMS08].

4 Block SPD coupling manifold

We propose the following Riemannian manifold structure, termed as the block SPD coupling manifold,

$$\mathcal{M}_{m,n}^d(\mathbf{P}, \mathbf{Q}) := \{\Gamma : \Gamma_{i,j} \in \mathbb{S}_{++}^d, \sum_j \Gamma_{i,j} = \mathbf{P}_i, \sum_i \Gamma_{i,j} = \mathbf{Q}_j\}, \quad (3)$$

where $\sum_i \mathbf{P}_i = \sum_j \mathbf{Q}_j = \mathbf{I}$. Particularly, we restrict $\mathbf{P}_i, \mathbf{Q}_j, \Gamma_{i,j} \in \mathbb{S}_{++}^d$, the set of SPD matrices. This ensures that the proposed manifold $\mathcal{M}_{m,n}^d(\mathbf{P}, \mathbf{Q})$ in (3) is the interior of the set $\Pi(m, n, d, \mathbf{P}, \mathbf{Q})$.

For arbitrary SPD marginals \mathbf{P}, \mathbf{Q} , there is no guarantee that the set $\mathcal{M}_{m,n}^d(\mathbf{P}, \mathbf{Q})$ defined in (3) is non-empty [NGT14]. Hence, we assume the following.

Assumption 4.1. The block-SPD marginals \mathbf{P} and \mathbf{Q} are chosen such that there exists at least one element in the set $\mathcal{M}_{m,n}^d(\mathbf{P}, \mathbf{Q})$.

It should be noted that Assumption 4.1 can be easily satisfied for various types of block-SPD marginals such as uniform or arbitrary positive diagonal marginals.

Proposition 4.2. *Under Assumption 4.1, the set $\mathcal{M}_{m,n}^d(\mathbf{P}, \mathbf{Q})$ is smooth, i.e., differentiable.*

Proposition 4.2 implies that we can endow $\mathcal{M}_{m,n}^d(\mathbf{P}, \mathbf{Q})$ with a Riemannian structure (introduced in Section 4.1).

It should be emphasized that the proposed manifold $\mathcal{M}_{m,n}^d(\mathbf{P}, \mathbf{Q})$ can be regarded as a generalization to existing manifold structures. For example, when $d = 1$ and either $m = 1$ or $n = 1$, $\mathcal{M}_{m,n}^d(\mathbf{P}, \mathbf{Q})$ reduces to the multinomial manifold of probability simplex [SGH⁺15]. When $d = 1$ and $m, n \neq 1$, it becomes the so-called doubly stochastic manifold [DH19] with uniform marginals or

Algorithm 1 Riemannian optimization for solving (4).

- 1: Initialize a feasible $\mathbf{\Gamma} \in \mathcal{M}_{m,n}^d$.
 - 2: **while** not converging **do**
 - 3: Compute Riemannian gradient (and Hessian) at $\mathbf{\Gamma}$.
 - 4: Compute the update step $\boldsymbol{\xi} \in T_{\mathbf{\Gamma}}\mathcal{M}_{m,n}^d$.
 - 5: Update $\mathbf{\Gamma} \leftarrow R_{\mathbf{\Gamma}}(\boldsymbol{\xi})$.
 - 6: **end while**
-

the more general matrix coupling manifold [SGH⁺21]. When $d > 1$ and either $m = 1$ or $n = 1$, our proposed manifold simplifies to the simplex manifold of SPD matrices [MKJ19].

Below, we derive various optimization-related ingredients on $\mathcal{M}_{m,n}^d(\mathbf{P}, \mathbf{Q})$ that allow optimization of an arbitrary differentiable objective function on the manifold. It follows the general treatment proposed by [AMS08].

4.1 Riemannian geometry and optimization on $\mathcal{M}_{m,n}^d$

We consider the general problem

$$\min_{\mathbf{\Gamma} \in \mathcal{M}_{m,n}^d(\mathbf{P}, \mathbf{Q})} F(\mathbf{\Gamma}) \quad (4)$$

via the Riemannian optimization framework. It provides a principled class of optimization methods and computational tools for manifolds, both first order and second order, as long as the ingredients such as Riemannian metric, orthogonal projection, retraction, and Riemannian gradient (and Hessian) of a function are defined [AMS08, BMAS14, Bou20]. Conceptually, the Riemannian optimization framework treats (4) as an “unconstrained” optimization problem over the constraint manifold $\mathcal{M}_{m,n}^d$ (omitted marginals \mathbf{P}, \mathbf{Q} for clarity).

In Algorithm 1, we outline the skeletal steps involved in optimization over $\mathcal{M}_{m,n}^d$, where the step $\boldsymbol{\xi}$ can be computed from different Riemannian methods. In Riemannian steepest descent, $\boldsymbol{\xi} = -\eta \text{grad}F(\mathbf{\Gamma})$, where $\text{grad}F(\mathbf{\Gamma})$ is the Riemannian gradient at $\mathbf{\Gamma}$ and η is step size. Also, $\boldsymbol{\xi}$ is given by the “conjugate” direction of $\text{grad}F(\mathbf{\Gamma})$ in the Riemannian conjugate gradient method. And, for the Riemannian trust-region method, $\boldsymbol{\xi}$ computation involves minimizing a second-order approximation of the objective function in a trust-region ball [AMS08]. Below, we show the computations of these ingredients.

Riemannian metric. The manifold $\mathcal{M}_{m,n}^d$ is a submanifold of the Cartesian product of $m \times n$ SPD manifold of size $d \times d$, which we denote as $\times_{m,n} \mathbb{S}_{++}^d$. The dimension of the manifold $\mathcal{M}_{m,n}^d$ is $(m-1)(n-1)d(d+1)/2$. The tangent space characterization of $\mathcal{M}_{m,n}^d$ at $\mathbf{\Gamma}$ is given by

$$T_{\mathbf{\Gamma}}\mathcal{M}_{m,n}^d = \{[\mathbf{U}_{i,j}]_{m \times n} : \mathbf{U}_{i,j} \in \mathbb{S}^d, \sum_j \mathbf{U}_{i,j} = \mathbf{0}, \sum_i \mathbf{U}_{i,j} = \mathbf{0}\},$$

where \mathbb{S}^d is the set of $d \times d$ symmetric matrices. We endow each SPD manifold with the affine-invariant Riemannian metric [Bha09], which induces a Riemannian metric for the product manifold $\mathcal{M}_{m,n}^d$ as

$$\langle \mathbf{U}, \mathbf{V} \rangle_{\mathbf{\Gamma}} = \sum_{i,j} \text{tr}(\mathbf{\Gamma}_{i,j}^{-1} \mathbf{U}_{i,j} \mathbf{\Gamma}_{i,j}^{-1} \mathbf{V}_{i,j}), \quad (5)$$

for any $\mathbf{U}, \mathbf{V} \in T_{\Gamma} \mathcal{M}_{m,n}^d$.

Orthogonal projection, Riemannian gradient, and Riemannian Hessian. As an embedded submanifold, the orthogonal projection plays a crucial role in deriving the Riemannian gradient (as orthogonal projection of the Euclidean gradient in the ambient space).

Proposition 4.3. *The orthogonal projection of any $\mathbf{S} \in \times_{m,n} \mathbb{S}^d$ to $T_{\Gamma} \mathcal{M}_{m,n}^d$ with respect to the Riemannian metric (5) is given by*

$$\mathbf{P}_{\Gamma}(\mathbf{S}) = \mathbf{U}, \text{ with } \mathbf{U}_{i,j} = \mathbf{S}_{i,j} + \Gamma_{i,j}(\Lambda_i + \Theta_j)\Gamma_{i,j},$$

where auxiliary variables Λ_i, Θ_j are solved from the system of matrix linear equations:

$$\begin{cases} -\sum_i \mathbf{S}_{i,j} = \sum_i \Gamma_{i,j}(\Lambda_i + \Theta_j)\Gamma_{i,j}, & \forall j \\ -\sum_j \mathbf{S}_{i,j} = \sum_j \Gamma_{i,j}(\Lambda_i + \Theta_j)\Gamma_{i,j}, & \forall i. \end{cases}$$

Subsequently, the Riemannian gradient and Hessian are derived as the orthogonal projection of the gradient and Hessian from the ambient space.

Proposition 4.4. *The Riemannian gradient and Hessian of $F : \mathcal{M}_{m \times n}^d \rightarrow \mathbb{R}$ are derived as*

$$\begin{aligned} \text{grad}F(\Gamma) &= \mathbf{P}_{\Gamma}([\Gamma_{i,j}\{\nabla F(\Gamma_{i,j})\}_S\Gamma_{i,j}]_{m \times n}), \\ \text{Hess}F(\Gamma)[\mathbf{U}] &= \mathbf{P}_{\Gamma}([\text{Dgrad}F(\Gamma_{i,j})[\mathbf{U}_{i,j}] - \{\mathbf{U}_{i,j}\Gamma_{i,j}^{-1}\text{grad}F(\Gamma_{i,j})\}_S]_{m \times n}), \end{aligned}$$

where $\mathbf{U} \in T_{\Gamma} \mathcal{M}_{m,n}^d$ and $\nabla F(\Gamma_{i,j})$ is the block partial derivative of F with respect to $\Gamma_{i,j}$. Here, $\text{Dgrad}F(\Gamma_{i,j})[\mathbf{U}_{i,j}]$ denotes the directional derivative of the Riemannian gradient $\text{grad}F$ along \mathbf{U} and $\{\mathbf{A}\}_S := (\mathbf{A} + \mathbf{A}^{\top})/2$.

Retraction and block matrix balancing algorithm. Retraction of $\mathcal{M}_{m,n}^d$ is given by a composition of two operations. The first operation is to ensure positive definiteness of the blocks in the coupling matrix. In particular, we use the exponential map associated with the affine-invariant metric on the SPD manifold \mathbb{S}_{++}^d [Bha09]. The second operation is to ensure that the summation of the row blocks and column blocks respect the block-SPD marginals. Given an initialized block SPD matrix $[\mathbf{A}_{i,j}]_{m \times n}$, where $\mathbf{A}_{i,j} \in \mathbb{S}_{++}^d$, the goal is to find a ‘closest’ block SPD coupling matrix $\mathbf{B} \in \mathcal{M}_{m,n}^d$. This is achieved by alternatively normalizing the row and column blocks to the corresponding marginals. The procedure is outlined in Algorithm 2. The solution for the row and column normalization factors $\mathbf{R}_j, \mathbf{L}_i$, which are SPD matrices, are computed by solving the Riccati equation $\mathbf{T}\mathbf{X}\mathbf{T} = \mathbf{Y}$ for given $\mathbf{X}, \mathbf{Y} \in \mathbb{S}_{++}^d$. Here, \mathbf{T} admits a unique solution [Bha09, MMP18]. Different from the scalar marginals case where the scaling can be expressed as a diagonal matrix, we need to symmetrically normalize each SPD block matrix. Algorithm 2 is a generalization of the RAS algorithm for balancing non-negative matrices [Sin67], which is related to the popular Sinkhorn-Knopp algorithm [Sin64, Kni08].

It should be noted that a similar matrix balancing algorithm has been introduced for positive operators [Gur04, GP15], where the convergence is only established in limited cases. Algorithm 2 is different from the quantum Sinkhorn algorithm proposed in [PCVS19] that applies to the unbalanced setting. Although we do not provide a theoretical convergence analysis for Algorithm 2, we empirically observe quick convergence of this algorithm in various settings (see Appendix A).

Algorithm 2 Block matrix balancing algorithm

- 1: **Input:** $[\mathbf{A}_{i,j}]_{m \times n}$, where $\mathbf{A}_{i,j} \in \mathbb{S}_{++}^d$.
 - 2: **while** not converging **do**
 - 3: Find $\mathbf{R}_j \in \mathbb{S}_{++}^d$ such that $\sum_i \mathbf{R}_j \mathbf{A}_{i,j} \mathbf{R}_j = \mathbf{Q}_j, \forall j$.
 - 4: Update $\mathbf{A}_{i,j} \leftarrow \mathbf{R}_j \mathbf{A}_{i,j} \mathbf{R}_j, \forall j$.
 - 5: Find $\mathbf{L}_i \in \mathbb{S}_{++}^d$ such that $\sum_j \mathbf{L}_i \mathbf{A}_{i,j} \mathbf{L}_i = \mathbf{P}_i, \forall i$.
 - 6: Update $\mathbf{A}_{i,j} \leftarrow \mathbf{L}_i \mathbf{A}_{i,j} \mathbf{L}_i, \forall i$.
 - 7: **end while**
 - 8: **Output:** The balanced matrix $\mathbf{B} = \mathbf{A}$.
-

Based on Algorithm 2, we define a retraction $R_{\mathbf{\Gamma}}(\mathbf{U})$ at $\mathbf{\Gamma} \in \mathcal{M}_{m,n}^d$ for any $\mathbf{U} \in T_{\mathbf{\Gamma}}\mathcal{M}_{m,n}^d$ as

$$R_{\mathbf{\Gamma}}(\mathbf{U}) = \text{MBalance}([\mathbf{\Gamma}_{i,j} \exp(\mathbf{\Gamma}_{i,j}^{-1} \mathbf{U}_{i,j})]_{m \times n}), \quad (6)$$

where MBalance calls the matrix balancing procedure in Algorithm 2 and $\exp(\cdot)$ denotes the matrix exponential. The retraction proposed in (6) is valid (i.e., satisfy the two conditions) for diagonal marginals and empirically we also see the retraction is well-defined for arbitrary block-SPD marginals. See Appendix A for more details.

4.2 Convergence and computational complexity

Convergence of Riemannian optimization. Similar to Euclidean optimization, the necessary first-order optimality condition for any differentiable F on $\mathcal{M}_{m,n}^d$ is $\text{grad}F(\mathbf{\Gamma}^*) = 0$, i.e., where the Riemannian gradient vanishes. We call such $\mathbf{\Gamma}^*$ the stationary point. The Riemannian methods are known to converge to a stationary point [AMS08, Bou20] under standard assumptions. Additionally, we show the following.

Theorem 4.5. *Suppose the objective function of the problem $\min_{\mathbf{\Gamma} \in \Pi(m,n,d,\mathbf{P},\mathbf{Q})} F(\mathbf{\Gamma})$ is (strictly) convex and the optimal solution $\mathbf{\Gamma}^*$ is positive definite, i.e., it lies in the interior of $\Pi(m,n,d,\mathbf{P},\mathbf{Q})$. Then, Riemannian optimization (Algorithm 1) for (4) converges to the same global optimal solution $\mathbf{\Gamma}^*$.*

Theorem 4.5 guarantees the quality of the solution obtained by Riemannian optimization for a class of objective functions which includes the SPD matrix-valued OT problem with convex regularization.

Computational complexity. The complexity of each iteration of the Riemannian optimization algorithm is dominated by the computations of retraction and the Riemannian gradient (and Hessian). These also make use of the orthogonal projection operation. All these operations cost $O(mnd^3)$. It should be noted that the number of parameters to be learned is mnd^2 .

5 Extensions of block SPD optimal transport

In this section, we discuss extensions of the proposed SPD OT framework to Wasserstein barycenters and the Gromov-Wasserstein setting.

5.1 Block SPD Wasserstein barycenter learning

We consider the problem of computing the Wasserstein barycenter of a set of block SPD matrix-valued measures. Let $\Delta_n(\mathbb{S}_{++}^d) := \{\mathbf{P} = [\mathbf{P}_i]_{n \times 1} : \mathbf{P}_i \in \mathbb{S}_{++}^d, \sum_i \mathbf{P}_i = \mathbf{I}\}$ denotes the space of $n \times 1$ block SPD marginals. Then, the Wasserstein barycenter $\bar{\mathbf{P}}$ of a set $\{\mathbf{P}^\ell\}_{\ell=1}^K \in \Delta_n(\mathbb{S}_{++}^d)$ is computed as follows:

$$\bar{\mathbf{P}} = \arg \min_{\mathbf{P} \in \Delta_n(\mathbb{S}_{++}^d)} \sum_{\ell=1}^K \omega_\ell \text{MW}_\epsilon^2(\mathbf{P}, \mathbf{P}^\ell), \quad (7)$$

where the given non-negative weights satisfy $\sum_\ell \omega_\ell = 1$. It should be noted that we employ a regularized version of the proposed block SPD OT problem (2) to ensure the differentiability of the objective function near boundary in (7). The regularized block SPD OT problem is defined as

$$\text{MW}_\epsilon^2(\mathbf{P}, \mathbf{Q}) := \min_{\Gamma \in \mathcal{M}_{m,n}^d(\mathbf{P}, \mathbf{Q})} \sum_{i,j} \left(\text{tr}(\mathbf{C}_{i,j} \Gamma_{i,j}) + \epsilon \Omega(\Gamma_{i,j}) \right), \quad (8)$$

where $\epsilon > 0$ is the regularization parameter and $\Omega(\cdot)$ is a strictly convex regularization (e.g., entropic regularization) on the block SPD coupling matrices.

To solve for $\bar{\mathbf{P}}$ in (7), we consider Riemannian optimization on $\Delta_n(\mathbb{S}_{++}^d)$, which has recently been studied in [MKJ19]. The following result provides an expression for the Euclidean gradient of the objective function in problem (7).

Proposition 5.1. *The Euclidean gradient of (7) with respect to \mathbf{P}_i , for $i \in [n]$ is*

$$\sum_{\ell=1}^K \omega_\ell \nabla_{\mathbf{P}_i} \text{MW}_\epsilon(\mathbf{P}, \mathbf{P}^\ell) = - \sum_{\ell=1}^K \omega_\ell (\mathbf{\Lambda}_i^\ell)^*,$$

where $(\mathbf{\Lambda}_i^\ell)^*$ is given by evaluating the orthogonal projection $\mathbf{P}_{(\Gamma^\ell)^*}(\nabla_{(\Gamma^\ell)^*} \text{MW}_\epsilon)$, with $\nabla_{(\Gamma_{i,j}^\ell)^*} \text{MW}_\epsilon = \mathbf{C}_{i,j}^\ell + \epsilon \nabla \Omega((\Gamma_{i,j}^\ell)^*)$ and $(\Gamma^\ell)^*$ is the optimal coupling for \mathbf{P}^ℓ . That is, $(\mathbf{\Lambda}_i^\ell)^*$ is the auxiliary variable obtained during the solving of the system of matrix linear equations in Proposition 4.3.

The algorithm for computing the barycenter in (7) is outlined in Algorithm 3 (Appendix G).

5.2 Block SPD Gromov-Wasserstein discrepancy

The Gromov-Wasserstein (GW) distance [Mém11] generalizes the optimal transport to the case where the measures are supported on possibly different metric spaces \mathcal{X} and \mathcal{Y} . Let $\mathbf{D}^x \in \mathbb{R}^{m \times m}$ and $\mathbf{D}^y \in \mathbb{R}^{n \times n}$ represent the similarity (or distance) between elements in metric spaces \mathcal{X} and \mathcal{Y} respectively. Let $\mathbf{p} \in \Sigma_m$ and $\mathbf{q} \in \Sigma_n$ be the marginals corresponding to the elements in \mathcal{X} and \mathcal{Y} , respectively. Then, the GW discrepancy between the two distance-marginal pairs $(\mathbf{D}^x, \mathbf{p})$ and $(\mathbf{D}^y, \mathbf{q})$ is defined as

$$\text{GW}((\mathbf{D}^x, \mathbf{p}), (\mathbf{D}^y, \mathbf{q})) := \min_{\gamma \in \Pi(\mathbf{p}, \mathbf{q})} \sum_{i,i',j,j'} \mathcal{L}(D_{i,i'}^x, D_{j,j'}^y) \gamma_{i,j} \gamma_{i',j'},$$

where $D_{k,l}$ denotes the (k, l) -th element in the matrix \mathbf{D} and \mathcal{L} is a loss between the distance pairs. Common choices of \mathcal{L} include the L_2 distance and the KL divergence.

We now generalize the GW framework to our setting where the marginals are SPD matrix-valued measures. Let $(\mathbf{D}^x, \mathbf{P})$ and $(\mathbf{D}^y, \mathbf{Q})$ be two distance-marginal pairs, where the Dirac measures

are given by $\sum_i \mathbf{P}_i \delta_{x_i}$, $\sum_j \mathbf{Q}_j \delta_{y_j}$ respectively, for $\{x_i\}_{i \in [m]} \subset \mathcal{X}$, $\{y_j\}_{j \in [n]} \subset \mathcal{Y}$. The marginals are tensor-valued with $\mathbf{P} \in \Delta_m(\mathbb{S}_{++}^d)$, $\mathbf{Q} \in \Delta_n(\mathbb{S}_{++}^d)$. We define the SPD generalized GW discrepancy as

$$\text{MGW}((\mathbf{D}^x, \mathbf{P}), (\mathbf{D}^y, \mathbf{Q})) := \min_{\Gamma \in \mathcal{M}_{m \times n}^d} \sum_{i,i',j,j'} \mathcal{L}(D_{i,i'}^x, D_{j,j'}^y) \text{tr}(\Gamma_{i,j} \Gamma_{i',j'}), \quad (9)$$

where we use Riemannian optimization (Algorithm 1) to solve problem (9).

Gromov-Wasserstein averaging of distance matrices. The GW formulation with scalar-valued probability measures has been used for averaging distance matrices [PCS16]. Building on (9), we consider the problem of averaging distance matrices where the marginals are SPD-valued. Let $\{(\mathbf{D}^\ell, \mathbf{P}^\ell)\}_{\ell=1}^K$ with $\mathbf{P}^\ell \in \Delta_{n_\ell}(\mathbb{S}_{++}^d)$, be a set of distance-marginal pairs on K incomparable domains. Suppose the barycenter marginals $\bar{\mathbf{P}} \in \Delta_n(\mathbb{S}_{++}^d)$ are given, the goal is to find the average distance matrix $\bar{\mathbf{D}}$ by solving

$$\bar{\mathbf{D}} = \arg \min_{\mathbf{D} \in \mathbb{S}^n: D_{i,j} \geq 0} \sum_{\ell=1}^K \omega_\ell \text{MGW}((\mathbf{D}, \bar{\mathbf{P}}), (\mathbf{D}^\ell, \mathbf{P}^\ell)), \quad (10)$$

where the given weights satisfy $\sum_\ell \omega_\ell = 1$. Problem (10) can be solved via a block coordinate descent method, that iteratively updates the couplings $\{\Gamma^\ell\}_{\ell=1}^K$ and the distance matrix $\bar{\mathbf{D}}$. The update of the coupling is performed via Algorithm 1. For the update of the distance matrix, we show when the loss \mathcal{L} is decomposable, including the case of L_2 distance or the KL divergence, the optimal $\bar{\mathbf{D}}$ admits a closed-form solution. This is a generalization of the result [PCS16, Proposition 3] to SPD-valued marginals.

Proposition 5.2. *Suppose the loss \mathcal{L} can be decomposed as $\mathcal{L}(a, b) = f_1(a) + f_2(b) - h_1(a)h_2(b)$ with f'_1/h'_1 invertible, then (10) has a closed form solution given by $\bar{D}_{i,i'} = \left(\frac{f'_1}{h'_1}\right)^{-1}(h_{i,i'})$ with*

$$h_{i,i'} = \left(\frac{\sum_{\ell=1}^K \omega_\ell \text{tr} \left(\sum_j \Gamma_{i,j}^\ell \sum_{j'} h_2(D_{j,j'}^\ell) \Gamma_{i',j'}^\ell \right)}{\text{tr}(\bar{\mathbf{P}}_i \bar{\mathbf{P}}_{i'})} \right).$$

6 Experiments

In this section, we show the utility of the proposed framework in a number of applications. For empirical comparisons, we refer to our approaches, block SPD OT (2), the corresponding Wasserstein barycenter (7), and block SPD Gromov-Wasserstein OT (9) & (10), collectively as RMOT (Riemannian optimized Matrix Optimal Transport). For all the experiments, we use the Riemannian steepest descent method using the Manopt toolbox [BMAS14] in Algorithm 1.

The code can be found on <https://github.com/andyjm3/BlockSPDOT>.

6.1 Domain adaptation

We apply our OT framework to the application of unsupervised domain adaptation where the goal is to align the distribution of the source with the target for subsequent tasks.

Suppose we are given the source $\mathbf{p} \in \Sigma_m$ and target marginals $\mathbf{q} \in \Sigma_n$, along with samples $\{\mathbf{X}_i\}_{i=1}^m$, $\{\mathbf{Y}_j\}_{j=1}^n$ from the source and target distributions. The samples are matrix-valued, i.e., $\mathbf{X}_i, \mathbf{Y}_j \in \mathbb{R}^{d \times s}$. We define the cost as $\mathbf{C}_{i,j} = (\mathbf{X}_i - \mathbf{Y}_j)(\mathbf{X}_i - \mathbf{Y}_j)^\top$. It should be noted that

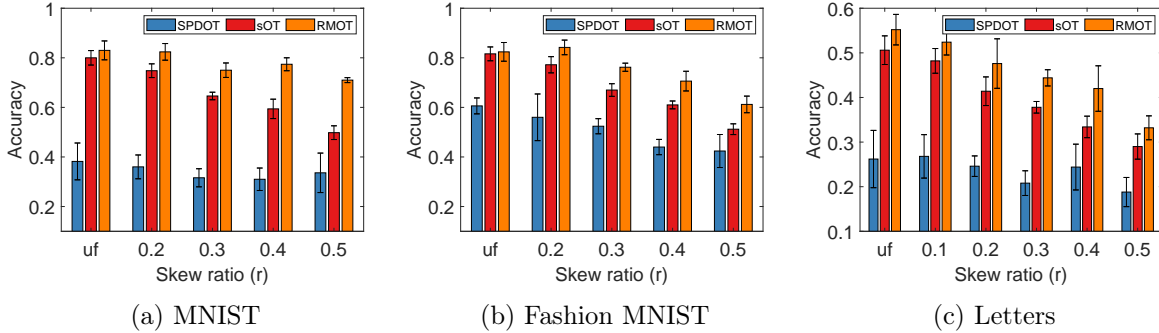


Figure 1: Domain adaptation and classification results for three datasets: MNIST (1a), Fashion MNIST (1b) and Letters (1c). The skew ratio increases from uniform (uf) to $r = 0.5$. For MNIST and Fashion MNIST, $uf = 0.1$ and for Letters, $uf = 1/26$. We observe that the proposed RMOT performs significantly better than the baselines.

$\text{tr}(\mathbf{C}_{i,j}) = \|\mathbf{X}_i - \mathbf{Y}_j\|_{\mathbb{F}}^2$, which is the cost function under the 2-Wasserstein OT setting (1). For domain adaptation, we first learn an optimal coupling between the source and target samples by solving the proposed OT problem (2) with marginals \mathbf{P}, \mathbf{Q} constructed as $\mathbf{P} := \{[\mathbf{P}_i]_{m \times 1} : \mathbf{P}_i = p_i \mathbf{I}\}$ and $\mathbf{Q} := \{[\mathbf{Q}_j]_{n \times 1} : \mathbf{Q}_j = q_j \mathbf{I}\}$ (as discussed in Section 3). Finally, the source samples are projected to the target domain via barycentric projection.

With the optimal coupling $\Gamma_{i,j}^*$, the barycentric projection of a source sample \mathbf{X}_i is computed as

$$\hat{\mathbf{X}}_i = \arg \min_{\mathbf{X}_i \in \mathbb{R}^{d \times s}} \sum_{i,j} \text{tr}((\mathbf{X}_i - \mathbf{Y}_j)(\mathbf{X}_i - \mathbf{Y}_j)^\top \Gamma_{i,j}^*) = \mathbf{P}_i^{-1} \left(\sum_j \Gamma_{i,j}^* \mathbf{Y}_j \right).$$

The above formulation also works for structured samples. For instance, when the samples are SPD, i.e., $\mathbf{X}_i, \mathbf{Y}_j \in \mathbb{S}_{++}^d$, the projected source sample $\hat{\mathbf{X}}_i$ is now the solution to the matrix Lyapunov equation: $\{\mathbf{P}_i \hat{\mathbf{X}}_i\}_s = \{\sum_j \Gamma_{i,j}^* \mathbf{Y}_j\}_s$. Here, $\{\mathbf{A}\}_s = (\mathbf{A} + \mathbf{A}^\top)/2$.

Experimental setup. We employ domain adaptation to classify the test sets (target) of multiclass image datasets, where the training sets (source) have a different class distribution than the test sets. Suppose we are given a training set $\{\mathbf{X}_i\}_{i=1}^m$ and a test set $\{\mathbf{Y}_j\}_{j=1}^n$ where $\mathbf{X}_i, \mathbf{Y}_j \in \mathbb{R}^{d \times s}$ are s (normalized) image samples of the same class in d dimension for each image set i, j . Instead of constructing the cost directly on the input space, which are not permutation-invariant, we first compute the sample covariances $\mathbf{S}_{x_i} = \mathbf{X}_i \mathbf{X}_i^\top / s$ and $\mathbf{S}_{y_j} = \mathbf{Y}_j \mathbf{Y}_j^\top / s, \forall i, j$. Now the cost between i, j is given by $\mathbf{C}_{i,j} = (\mathbf{S}_{x_i} - \mathbf{S}_{y_j})(\mathbf{S}_{x_i} - \mathbf{S}_{y_j})^\top$. Once the block SPD matrix coupling is learnt, the \mathbf{S}_{x_i} covariances are projected using the barycentric projection to obtain $\hat{\mathbf{S}}_{x_i}, i \in [m]$. This is followed by nearest neighbour classification of j based on the Frobenius distance $\|\hat{\mathbf{S}}_{x_i} - \mathbf{S}_{y_j}\|_{\mathbb{F}}, \forall i, j$. We set $p_i = 1/m$ and $q_j = 1/n$.

We compare the proposed RMOT (2) with the following baselines: (i) sOT: the 2-Wasserstein OT (1) with the cost $c_{i,j} = \text{tr}(\mathbf{C}_{i,j}) = \|\mathbf{S}_{x_i} - \mathbf{S}_{y_j}\|_{\mathbb{F}}^2$ [CFTR16], and (ii) SPDOT: the 2-Wasserstein OT (1) with the cost as the squared Riemannian geodesic distance between the SPD matrices \mathbf{S}_{x_i} and \mathbf{S}_{y_j} [YBCT19].

Datasets. We experiment on three multiclass image datasets - handwritten letters [FS91], MNIST [LBBH98] and Fashion MNIST [XRV17] - with various skewed distributions for the training

set. MNIST and Fashion MNIST have 10 classes, while Letters has 26 classes. Specifically, we fix the distribution of the test set to be uniform (with the same number of image sets per class). We increase the proportion of the a randomly chosen class in the training set to the ratio r , where $r = \{\text{uf}, 0.1, 0.2, 0.3, 0.4, 0.5\}$ and uf is the ratio corresponding to the uniform distribution of all classes. We reduce the dimension of MNIST, fashion MNIST, and Letters by PCA to $d = 5$ features. We set $s = d$, $m = 250$, and $n = 100$ for each dataset.

Results. Figure 1 shows the classification accuracy on the three datasets. We observe that the proposed RMOT outperforms sOT and SPDOT, especially in more challenging domain adaptation settings, i.e., higher skew ratios. This shows the usefulness of the non-trivial correlations learned by the SPD matrix valued couplings of RMOT.

6.2 Tensor Gromov-Wasserstein distance averaging for shape interpolation

We consider an application of the proposed block SPD Gromov-Wasserstein OT formulation (Section 5.2) for interpolating tensor-valued shapes. We are given two distance-marginal pairs $(\mathbf{D}^0, \mathbf{P}^0), (\mathbf{D}^1, \mathbf{P}^1)$ where $\mathbf{D}^0, \mathbf{D}^1 \in \mathbb{R}^{n \times n}$ are distance matrices computed from the shapes and $\mathbf{P}^0, \mathbf{P}^1$ are given tensor fields. The aim is to interpolate between the distance matrices with weights $\omega = (t, 1 - t), t \in [0, 1]$. The interpolated distance matrix \mathbf{D}^t is computed by solving (10) via Riemannian optimization and Proposition 5.2, with the barycenter tensor fields \mathbf{P}^t given. Finally, the shape is recovered by performing multi-dimensional scaling to the distance matrix.

Figure 2 presents the interpolated shapes with $n = 100$ sample points for the input shapes. The matrices $\mathbf{D}^0, \mathbf{D}^1$ are given by the Euclidean distance and we consider L_2 loss for \mathcal{L} . The input tensor fields $\mathbf{P}^0, \mathbf{P}^1$ are generated as uniformly random in (a), cross-oriented in (b) and smoothly varying in (c). The barycenter tensor fields are given by the linear interpolation of the inputs, i.e., $\mathbf{P}^t = (1 - t)\mathbf{P}^0 + t\mathbf{P}^1$. The results show the proposed Riemannian optimization approach (Section 4) converges to reasonable stationary solutions for non-convex OT problems.

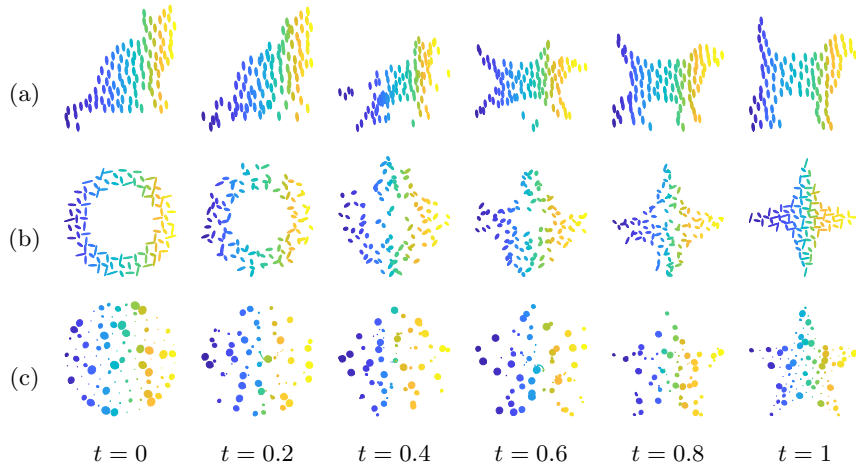


Figure 2: Tensor-valued shape interpolation obtained using the proposed RMOT (Section 5.2).

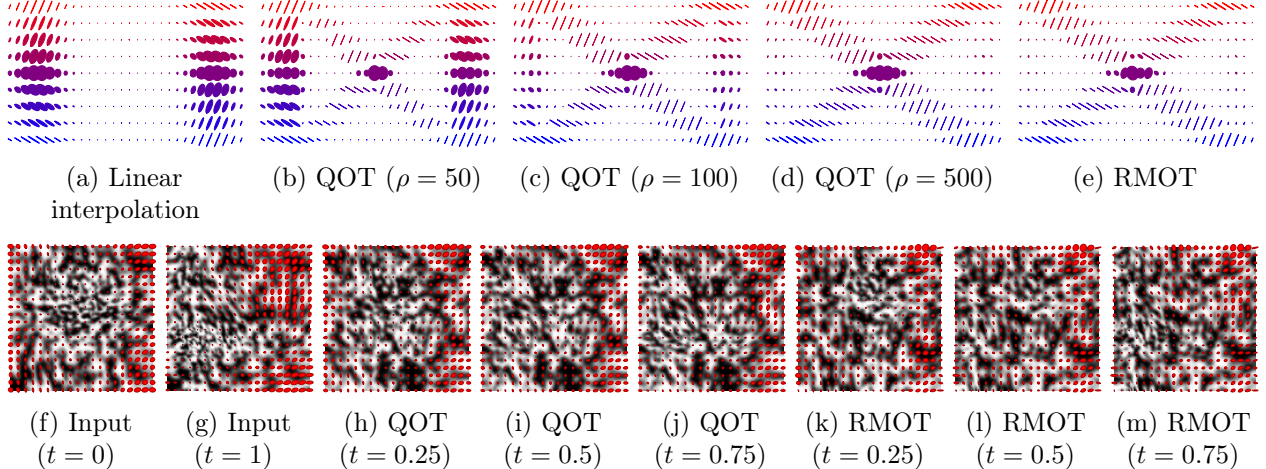


Figure 3: Tensor field mass interpolation on 1- d (top) and 2- d (bottom) grids. On the top, each row corresponds to an interpolation where we show 7 evenly-spaced interpolated tensor fields. On the bottom, the inputs are given in (f) and (g). We set $\rho = 100$ for QOT and show three evenly-spaced interpolated tensor fields.

6.3 Tensor field optimal transport mass interpolation

We consider performing optimal transport and displacement interpolation between two tensor fields supported on regular 1- d (or 2- d) grids [PCVS19]. We consider a common domain $\mathcal{D} = [0, 1]$ (or $[0, 1]^2$) with the cost defined as $\mathbf{C}_{i,j} = \|\mathbf{x}_i - \mathbf{y}_j\|^2 \mathbf{I}$ for $\mathbf{x}_i, \mathbf{y}_j \in \mathcal{D}$. The marginals \mathbf{P}, \mathbf{Q} are given tensor fields. We first compute the balanced coupling $\mathbf{\Gamma}$ by solving an entropy regularized OT problem (8):

$$\min_{\mathbf{\Gamma} \in \mathcal{M}_{m \times n}^d(\mathbf{P}, \mathbf{Q})} \sum_{i,j} \left(\text{tr}(\mathbf{C}_{i,j} \mathbf{\Gamma}_{i,j}) - \epsilon H(\mathbf{\Gamma}_{i,j}) \right),$$

where the quantum entropy is defined as $H(\mathbf{\Gamma}_{i,j}) := -\text{tr}(\mathbf{\Gamma}_{i,j} \log(\mathbf{\Gamma}_{i,j}) - \mathbf{\Gamma}_{i,j})$. Then, the coupling is used to interpolate between the two tensor fields by generalizing the displacement interpolation [McC97] to SPD-valued marginals. Please refer to [PCVS19, Section 2.2] for more details. It should be noted that due to the balanced nature of our formulation, we do not need to adjust the couplings after matching as required in [PCVS19].

We compare interpolation results of the proposed (balanced) RMOT with both linear interpolation $(1-t)\mathbf{P} + t\mathbf{Q}$ for $t \in [0, 1]$ and the *unbalanced* quantum OT (QOT) of [PCVS19]. The QOT solves the following problem with quantum KL regularization, i.e.,

$$\min_{\mathbf{\Gamma}} \sum_{i,j} \left(\text{tr}(\mathbf{C}_{i,j} \mathbf{\Gamma}_{i,j}) - \epsilon H(\mathbf{\Gamma}_{i,j}) + \rho \text{KL}(\mathbf{\Gamma} \mathbb{1} | \mathbf{P}) + \rho \text{KL}(\mathbf{\Gamma}^\top \mathbb{1} | \mathbf{Q}) \right),$$

where $\text{KL}(\mathbf{P} | \mathbf{Q}) := \sum_i \text{tr}(\mathbf{P}_i \log(\mathbf{P}_i) - \mathbf{P}_i \log(\mathbf{Q}_i) - \mathbf{P}_i + \mathbf{Q}_i)$ and $\mathbf{\Gamma} \mathbb{1} := [\sum_j (\mathbf{\Gamma}_{i,j})]_{m \times 1}$ and $\mathbf{\Gamma}^\top \mathbb{1} := [\sum_i (\mathbf{\Gamma}_{i,j})]_{n \times 1}$. For comparability, we set the same ϵ for both QOT and RMOT.

Figure 3 compares the mass interpolation for both 1- d (top) and 2- d (bottom) grids. For the 2- d tensor fields, we further renders the tensor fields via a background texture where we perform anisotropic smoothing determined by the tensor direction. In both the settings, we observe that the tensor fields generated from RMOT respect the marginal constraints more closely.



Figure 4: Barycenter interpolation. From left to right $t = 0$ (input), $t = 0.25, 0.5, 0.75$ (barycenters), $t = 1$ (input). The top row is QOT and the bottom is RMOT.

6.4 Tensor field Wasserstein barycenter

We also analyze the Wasserstein barycenters learned by the proposed RMOT approach and qualitatively compare with QOT barycenter [PCVS19, Section 4.1]. We test on two tensor fields ($n = 4$) supported 2- d grids.

Figure 4 compares barycenter from QOT (top) and RMOT (bottom) initialized from the normalized solution of QOT. We observe that the QOT solution is not optimal when the marginal constraint is enforced and the barycenter obtained does not lie in the simplex of tensors.

7 Conclusion

In this paper, we have discussed the balanced optimal transport (OT) problem involving SPD matrix-valued measures that is shown to be a natural generalization of 2-Wasserstein formulation. It also preserves the metric property. For the SPD matrix-valued OT problem, the coupling matrix is a block matrix where each block is a symmetric positive definite matrix. The set of such coupling matrices can be endowed with Riemannian geometry, which enables optimization of both linear and non-linear objective functions. We have also shown how the SPD-valued OT setup extend many optimal transport problems to general SPD-valued marginals, including the Wasserstein barycenter and the Gromov-Wasserstein (GW) discrepancy. Experiments in a number of applications confirm the benefit of our approach.

In the appendix Section E, we discuss the projected version of the SPD-valued OT problem. The robust version is shown to be a metric. As a future research direction, it would be interesting to explore such other properties. Another direction could be on learning of block coupling matrices with different constraints. In Section F, we discuss a constraint involving the matrix trace.

References

- [ABBC18] Naman Agarwal, Nicolas Boumal, Brian Bullins, and Coralia Cartis, *Adaptive regularization with cubics on manifolds*, arXiv:1806.00065 (2018).
- [ABG07] P-A Absil, Christopher G Baker, and Kyle A Gallivan, *Trust-region methods on riemannian manifolds*, Foundations of Computational Mathematics **7** (2007), no. 3, 303–330.
- [AMS08] P-A Absil, Robert Mahony, and Rodolphe Sepulchre, *Optimization algorithms on matrix manifolds*, Princeton University Press, 2008.

- [AP08] Yaniv Assaf and Ofer Pasternak, *Diffusion tensor imaging (DTI)-based white matter mapping in brain research: a review*, Journal of Molecular Neuroscience **34** (2008), no. 1, 51–61.
- [Bha09] Rajendra Bhatia, *Positive definite matrices*, Princeton University Press, 2009.
- [BMAS14] Nicolas Boumal, Bamdev Mishra, P-A Absil, and Rodolphe Sepulchre, *Manopt, a matlab toolbox for optimization on manifolds*, The Journal of Machine Learning Research **15** (2014), no. 1, 1455–1459.
- [Bou20] Nicolas Boumal, *An introduction to optimization on smooth manifolds*, Available online, Aug 2020.
- [CFT14] Nicolas Courty, Rémi Flamary, and Devis Tuia, *Domain adaptation with regularized optimal transport*, Joint European Conference on Machine Learning and Knowledge Discovery in Databases, Springer, 2014, pp. 274–289.
- [CFTR16] Nicolas Courty, Rémi Flamary, Devis Tuia, and Alain Rakotomamonjy, *Optimal transport for domain adaptation*, IEEE Transactions on Pattern Analysis and Machine Intelligence **39** (2016), no. 9, 1853–1865.
- [CGC⁺20] Liqun Chen, Zhe Gan, Yu Cheng, Linjie Li, Lawrence Carin, and Jingjing Liu, *Graph optimal transport for cross-domain alignment*, International Conference on Machine Learning, PMLR, 2020, pp. 1542–1553.
- [CGT17] Yongxin Chen, Tryphon T Georgiou, and Allen Tannenbaum, *Matrix optimal mass transport: a quantum mechanical approach*, IEEE Transactions on Automatic Control **63** (2017), no. 8, 2612–2619.
- [CGT18] ———, *Vector-valued optimal mass transport*, SIAM Journal on Applied Mathematics **78** (2018), no. 3, 1682–1696.
- [CM14] Eric A Carlen and Jan Maas, *An analog of the 2-Wasserstein metric in non-commutative probability under which the Fermionic Fokker–Planck equation is gradient flow for the entropy*, Communications in Mathematical Physics **331** (2014), no. 3, 887–926.
- [Cut13] Marco Cuturi, *Sinkhorn distances: Lightspeed computation of optimal transport*, Advances in Neural Information Processing Systems **26** (2013), 2292–2300.
- [DH19] Ahmed Douik and Babak Hassibi, *Manifold optimization over the set of doubly stochastic matrices: A second-order geometry*, IEEE Transactions on Signal Processing **67** (2019), no. 22, 5761–5774.
- [FS91] Peter W Frey and David J Slate, *Letter recognition using Holland-style adaptive classifiers*, Machine Learning **6** (1991), no. 2, 161–182.
- [GB14] Michael Grant and Stephen Boyd, *CVX: Matlab software for disciplined convex programming, version 2.1*, 2014.

- [GP15] Tryphon T Georgiou and Michele Pavon, *Positive contraction mappings for classical and quantum Schrödinger systems*, Journal of Mathematical Physics **56** (2015), no. 3, 033301.
- [Gur04] Leonid Gurvits, *Classical complexity and quantum entanglement*, Journal of Computer and System Sciences **69** (2004), no. 3, 448–484.
- [HSH14] Mehrtash T Harandi, Mathieu Salzmann, and Richard Hartley, *From manifold to manifold: Geometry-aware dimensionality reduction for SPD matrices*, European Conference on Computer Vision, Springer, 2014, pp. 17–32.
- [HWS⁺15] Zhiwu Huang, Ruiping Wang, Shiguang Shan, Xianqiu Li, and Xilin Chen, *Log-Euclidean metric learning on symmetric positive definite manifold with application to image set classification*, International Conference on Machine Learning, PMLR, 2015, pp. 720–729.
- [JNG12] Xianhua Jiang, Lipeng Ning, and Tryphon T Georgiou, *Distances and Riemannian metrics for multivariate spectral densities*, IEEE Transactions on Automatic Control **57** (2012), no. 7, 1723–1735.
- [Kni08] Philip A Knight, *The Sinkhorn–Knopp algorithm: convergence and applications*, SIAM Journal on Matrix Analysis and Applications **30** (2008), no. 1, 261–275.
- [LBBH98] Yann LeCun, Léon Bottou, Yoshua Bengio, and Patrick Haffner, *Gradient-based learning applied to document recognition*, Proceedings of the IEEE **86** (1998), no. 11, 2278–2324.
- [LBMP⁺01] Denis Le Bihan, Jean-François Mangin, Cyril Poupon, Chris A Clark, Sabina Pappata, Nicolas Molko, and Hughes Chabriat, *Diffusion tensor imaging: concepts and applications*, Journal of Magnetic Resonance Imaging **13** (2001), no. 4, 534–546.
- [McC97] Robert J McCann, *A convexity principle for interacting gases*, Advances in Mathematics **128** (1997), no. 1, 153–179.
- [Mém11] Facundo Mémoli, *Gromov–Wasserstein distances and the metric approach to object matching*, Foundations of Computational Mathematics **11** (2011), no. 4, 417–487.
- [MKJ19] Bamdev Mishra, Hiroyuki Kasai, and Pratik Jawanpuria, *Riemannian optimization on the simplex of positive definite matrices*, arXiv:1906.10436 (2019).
- [MMP18] Luigi Malagò, Luigi Montrucchio, and Giovanni Pistone, *Wasserstein Riemannian geometry of Gaussian densities*, Information Geometry **1** (2018), no. 2, 137–179.
- [MS16] Bamdev Mishra and Rodolphe Sepulchre, *Riemannian preconditioning*, SIAM Journal on Optimization **26** (2016), no. 1, 635–660.
- [MSDKJ21] Bamdev Mishra, NTV Satya Dev, Hiroyuki Kasai, and Pratik Jawanpuria, *Manifold optimization for optimal transport*, arXiv:2103.00902 (2021).

- [NGT14] Lipeng Ning, Tryphon T Georgiou, and Allen Tannenbaum, *On matrix-valued Monge–Kantorovich optimal mass transport*, IEEE Transactions on Automatic Control **60** (2014), no. 2, 373–382.
- [Nin13] L. Ning, *Matrix-valued optimal mass transportation and its applications*, Ph.D. thesis, University of Minnesota, 2013.
- [PC⁺19] Gabriel Peyré, Marco Cuturi, et al., *Computational optimal transport: With applications to data science*, Foundations and Trends® in Machine Learning **11** (2019), no. 5-6, 355–607.
- [PCS16] Gabriel Peyré, Marco Cuturi, and Justin Solomon, *Gromov–Wasserstein averaging of kernel and distance matrices*, International Conference on Machine Learning, PMLR, 2016, pp. 2664–2672.
- [PCVS19] Gabriel Peyré, Lenaïc Chizat, François-Xavier Vialard, and Justin Solomon, *Quantum entropic regularization of matrix-valued optimal transport*, European Journal of Applied Mathematics **30** (2019), no. 6, 1079–1102.
- [PMEGCF19] Hermina Petric Maretic, Mireille El Gheche, Giovanni Chierchia, and Pascal Frossard, *GOT: An optimal transport framework for graph comparison*, Advances in Neural Information Processing Systems **32** (2019), 13876–13887.
- [SDGP⁺15] Justin Solomon, Fernando De Goes, Gabriel Peyré, Marco Cuturi, Adrian Butscher, Andy Nguyen, Tao Du, and Leonidas Guibas, *Convolutional wasserstein distances: Efficient optimal transportation on geometric domains*, ACM Transactions on Graphics (TOG) **34** (2015), no. 4, 1–11.
- [SGH⁺15] Yanfeng Sun, Junbin Gao, Xia Hong, Bamdev Mishra, and Baocai Yin, *Heterogeneous tensor decomposition for clustering via manifold optimization*, IEEE Transactions on Pattern Analysis and Machine Intelligence **38** (2015), no. 3, 476–489.
- [SGH⁺21] Dai Shi, Junbin Gao, Xia Hong, ST Boris Choy, and Zhiyong Wang, *Coupling matrix manifolds assisted optimization for optimal transport problems*, Machine Learning **110** (2021), no. 3, 533–558.
- [Sin64] Richard Sinkhorn, *A relationship between arbitrary positive matrices and doubly stochastic matrices*, The Annals of Mathematical Statistics **35** (1964), no. 2, 876–879.
- [Sin67] ———, *Diagonal equivalence to matrices with prescribed row and column sums*, The American Mathematical Monthly **74** (1967), no. 4, 402–405.
- [SRGB14] Justin Solomon, Raif Rustamov, Leonidas Guibas, and Adrian Butscher, *Earth mover’s distances on discrete surfaces*, ACM Transactions on Graphics (TOG) **33** (2014), no. 4, 1–12.
- [Vil21] Cédric Villani, *Topics in optimal transportation*, vol. 58, American Mathematical Soc., 2021.
- [Wei98] Joachim Weickert, *Anisotropic diffusion in image processing*, vol. 1, Teubner Stuttgart, 1998.

- [XRV17] Han Xiao, Kashif Rasul, and Roland Vollgraf, *Fashion-mnist: a novel image dataset for benchmarking machine learning algorithms*, arXiv:1708.07747 (2017).
- [YBCT19] Or Yair, Mirela Ben-Chen, and Ronen Talmon, *Parallel transport on the cone manifold of spd matrices for domain adaptation*, IEEE Transactions on Signal Processing **67** (2019), no. 7, 1797–1811.
- [YCC⁺19] Mikhail Yurochkin, Sebastian Claiici, Edward Chien, Farzaneh Mirzazadeh, and Justin M Solomon, *Hierarchical optimal transport for document representation*, Advances in Neural Information Processing Systems **32** (2019), 1601–1611.

A Convergence of block matrix balancing algorithm and validity of retraction

In Section 4, we generalize the matrix scaling algorithm to the block matrix case, which is essential to derive the retraction operation for the manifold $\mathcal{M}_{m,n}^d$. Here, we empirically show that the algorithm quickly converges and the proposed retraction is valid and satisfies the two conditions: 1) $R_x(0) = x$ and 2) $DR_x(0)[u] = u$, where $Df(x)[u]$ is the derivative of a function at x along direction u [AMS08].

Convergence. We show in Figure 5 the convergence of the proposed block matrix balancing procedure in Algorithm 2. We generate the marginals as random SPD matrices for different dimensions d and size m, n . The convergence is measured as the relative gap to satisfy the constraints. We observe that the number of iterations for convergence are similar with different parameters while the runtime increases with increasing dimension and size.

Validity of retraction. The first condition of retraction is satisfied as $R_{\Gamma}(\mathbf{0}) = \text{MBalance}(\Gamma) = \Gamma$. For the second one, we have for any $\Gamma \in \mathcal{M}_{m,n}^d$ and $\mathbf{U} \in T_{\Gamma}\mathcal{M}_{m,n}^d$,

$$DR_{\Gamma}(\mathbf{0})[\mathbf{U}] = \lim_{h \rightarrow 0} \frac{R_{\Gamma}(h\mathbf{U}) - R_{\Gamma}(\mathbf{0})}{h}.$$

Hence, we need to numerically verify $R_{\Gamma}(h\mathbf{U}) - \Gamma = O(h)\mathbf{U}$ for any Γ, \mathbf{U} . To this end, we compute an approximation error in terms of the inner product on the tangent space $T_{\Gamma}\mathcal{M}_{m,n}^d$ as

$$\varepsilon = |\langle P_{\Gamma}(R_{\Gamma}(h\mathbf{U}) - \Gamma), \mathbf{V} \rangle_{\Gamma} - \langle h\mathbf{U}, \mathbf{V} \rangle_{\Gamma}|,$$

for any $\mathbf{V} \in T_{\Gamma}\mathcal{M}_{m,n}^d$ different from \mathbf{U} . In Figure 5(c), we show that the slope of the approximation error (as a function of h) matches the dotted line $h = 0$, which suggests that the error $\varepsilon = O(h)$, thereby indicating that the retraction is valid.

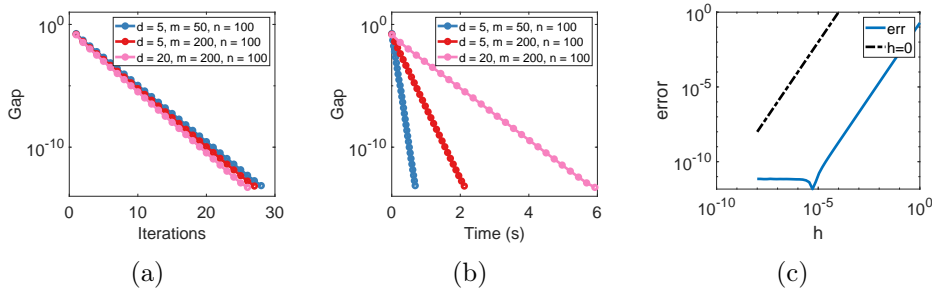


Figure 5: Convergence of Algorithm 2 in terms of iterations (a), runtime (b), and validity test for retraction (c). For the retraction to be valid, the slope of the continuous line should match the dotted line (which represents the line $h = 0$).

B Discussion on the construction of matrix-valued cost

As highlighted in Proposition 3.1, for $\text{MW}(\mathbf{p}, \mathbf{q})$ to be a metric, there are some conditions for the cost $[\mathbf{C}_{i,j}]_{m \times n}$ to satisfy. In the following, we give some examples of how such costs are constructed:

1. Let the samples are given by $\{\mathbf{X}_i\}_{i \in [m]}$, $\{\mathbf{Y}_j\}_{j \in [n]}$, where $\mathbf{X}_i, \mathbf{Y}_j \in \mathbb{R}^{d \times s}$. Define $\mathbf{C}_{i,j} = d(\mathbf{X}_i, \mathbf{Y}_j)^2 \mathbf{I}$, where $d: \mathbb{R}^{d \times s} \times \mathbb{R}^{d \times s} \rightarrow \mathbb{R}_+$ is a distance function.
2. Let the samples are given by $\{\mathbf{X}_i\}_{i \in [m]}$, $\{\mathbf{Y}_j\}_{j \in [n]}$, where $\mathbf{X}_i, \mathbf{Y}_j \in \mathbb{R}^{d \times s}$, where $s \geq d$. Assume the matrix $\mathbf{X}_i - \mathbf{Y}_j$ has column full rank. Define $\mathbf{C}_{i,j} = (\mathbf{X}_i - \mathbf{Y}_j)(\mathbf{X}_i - \mathbf{Y}_j)^\top$.

Proof. (1) The first definition of cost trivially satisfies all the conditions due to the metric properties of a well-defined scalar-valued distance.

(2) For the second definition of cost, The first two conditions, i.e., symmetric and positive definite conditions are easily satisfied and we only need to verify the third condition in Proposition 3.1. The third condition is also satisfied due to the triangle inequality of Mahalanobis distance metric in the vectorized form. That is, for any $\mathbf{A} \succeq \mathbf{0}$, we consider three sets of samples $\{\mathbf{X}_i\}, \{\mathbf{Y}_k\}, \{\mathbf{Z}_j\} \subset \mathbb{R}^{d \times s}$. Then we have

$$\begin{aligned}
\sqrt{\text{tr}(\mathbf{C}_{i,j} \mathbf{A})} &= \sqrt{\text{tr}((\mathbf{X}_i - \mathbf{Z}_j)^\top \mathbf{A} (\mathbf{X}_i - \mathbf{Z}_j))} \\
&= \sqrt{(\text{vec}(\mathbf{X}_i) - \text{vec}(\mathbf{Z}_j))^\top (\mathbf{I} \otimes \mathbf{A}) (\text{vec}(\mathbf{X}_i) - \text{vec}(\mathbf{Z}_j))} \\
&\leq \sqrt{(\text{vec}(\mathbf{X}_i) - \text{vec}(\mathbf{Y}_k))^\top (\mathbf{I} \otimes \mathbf{A}) (\text{vec}(\mathbf{X}_i) - \text{vec}(\mathbf{Y}_k))} \\
&\quad + \sqrt{(\text{vec}(\mathbf{Y}_k) - \text{vec}(\mathbf{Z}_j))^\top (\mathbf{I} \otimes \mathbf{A}) (\text{vec}(\mathbf{Y}_k) - \text{vec}(\mathbf{Z}_j))} \\
&= \sqrt{\text{tr}((\mathbf{X}_i - \mathbf{Y}_k)^\top \mathbf{A} (\mathbf{X}_i - \mathbf{Y}_k))} + \sqrt{\text{tr}((\mathbf{Y}_k - \mathbf{Z}_j)^\top \mathbf{A} (\mathbf{Y}_k - \mathbf{Z}_j))} \\
&= \sqrt{\text{tr}(\mathbf{C}_{i,k} \mathbf{A})} + \sqrt{\text{tr}(\mathbf{C}_{k,j} \mathbf{A})},
\end{aligned}$$

where $\text{vec}(\mathbf{C})$ denotes the vectorization of matrix \mathbf{C} by stacking the columns. □

C Additional experiments

In this section, we give additional experiments to further substantiate the claims made in the main text.

C.1 Tensor field optimal transport mass interpolation

In addition to the experiments presented in the main texts, we also show several other examples of tensor fields in Figures 6 and 7. Input-1 and Input-2 are with $t = 0$ and $t = 1$, respectively. QOT-2 and RMOT-2 are with $t = 0.25$. QOT-3 and RMOT-3 are with $t = 0.5$. QOT-4 and RMOT-4 are with $t = 0.75$.

C.2 Tensor field Wasserstein barycenter

We first show how both linear interpolation and QOT solutions are not optimal by comparing the objective value of $\sum_\ell \omega_\ell \text{MW}_\epsilon(\bar{\mathbf{P}}, \mathbf{P}^\ell)$ against the optimal objective, obtained from CVX [GB14]. This is achieved by initializing our Riemannian optimizers for $\bar{\mathbf{P}}$ from the linear interpolation and (normalized) QOT. We also include uniform initialization as a benchmark. In Figure 8, we see that the objective value keeps decreasing even after properly normalizing the barycenter.

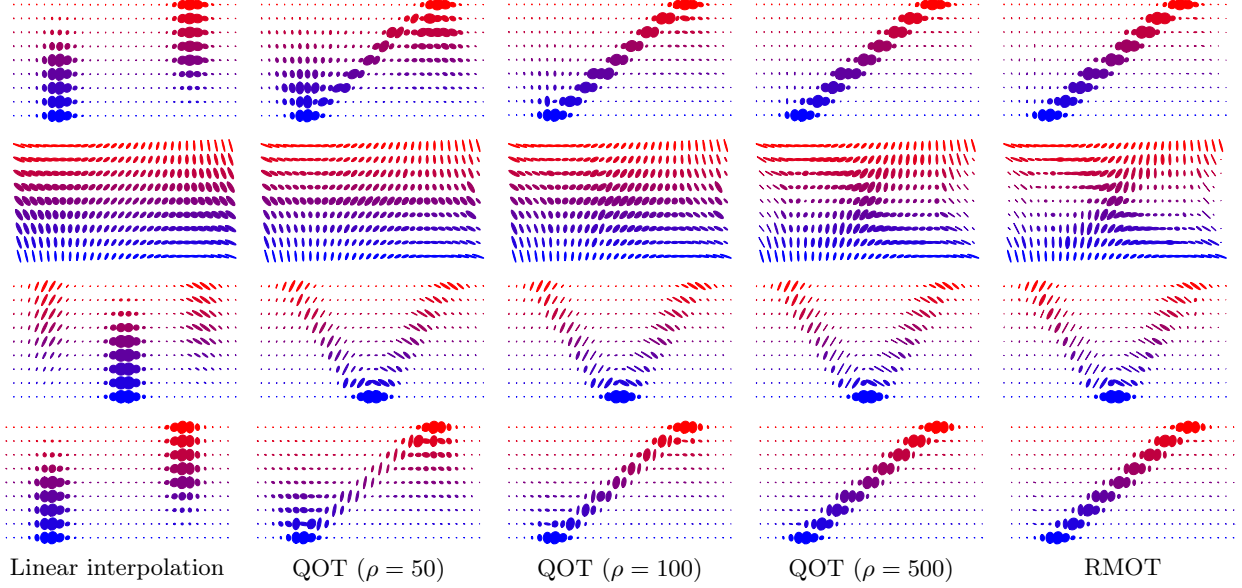


Figure 6: 1- d tensor fields mass interpolation.

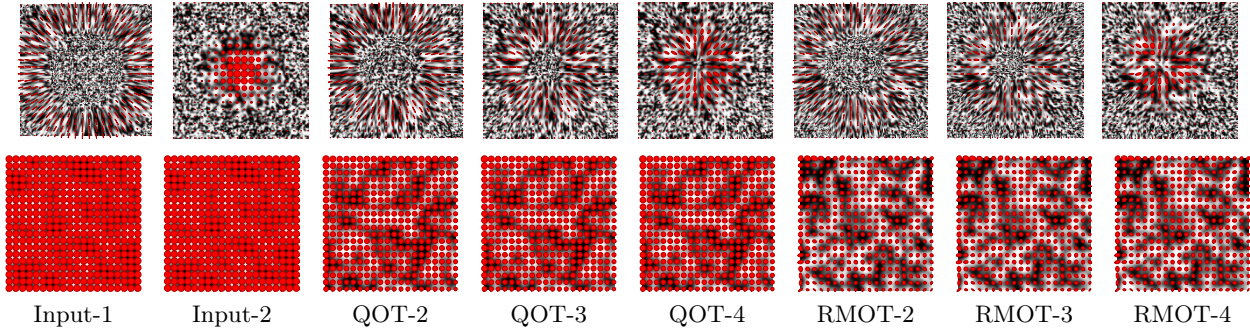


Figure 7: 2- d tensor fields mass interpolation.

Additionally, we show the barycenter results for $n = 16$ along with convergence with initialization from the QOT solution in Figure 9. Compared to the convergence where $n = 4$, the QOT solution is much closer to the optimal when $n = 16$.

D Proofs

Proof of Proposition 4.2. For a given feasible element $\mathbf{\Gamma} \in \mathcal{M}_{m,n}^d(\mathbf{P}, \mathbf{Q})$, we can construct a family of feasible elements. For example, choose $0 \leq \zeta < \min_{i,j} \{\lambda_{\min}(\mathbf{\Gamma}_{i,j})\}$. Then we can add/subtract the equal number of $\zeta \mathbf{I}$ and the result is still feasible. In other words, the set is smooth in an ball around the element $\mathbf{\Gamma}$ of radius ζ . \square

Proof of Proposition 3.1. For simplicity, we assume $\mathbf{p}, \mathbf{q} > 0$. Otherwise, we can follow [PC⁺19] to define $\tilde{p}_j = p_j$ if $p_j > 0$ and 1 otherwise. Then the proof proceeds.

First, it is easy to verify the symmetry property, i.e., $\text{MW}(\mathbf{p}, \mathbf{q}) = \text{MW}(\mathbf{q}, \mathbf{p})$. For the definiteness

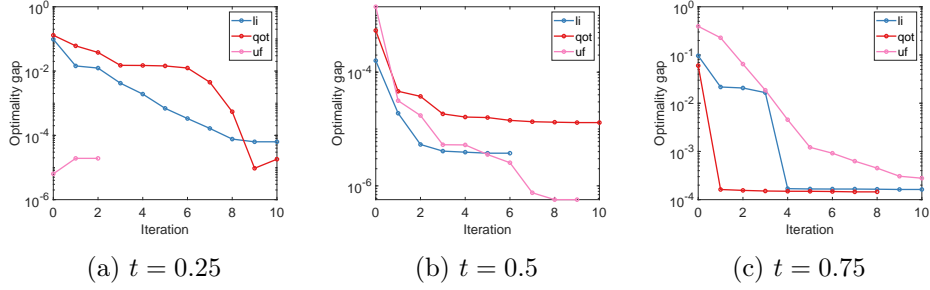


Figure 8: Convergence of ($n = 4$) barycenter update initialized from linear interpolation (li), QOT (qot), and uniform identity (uf).

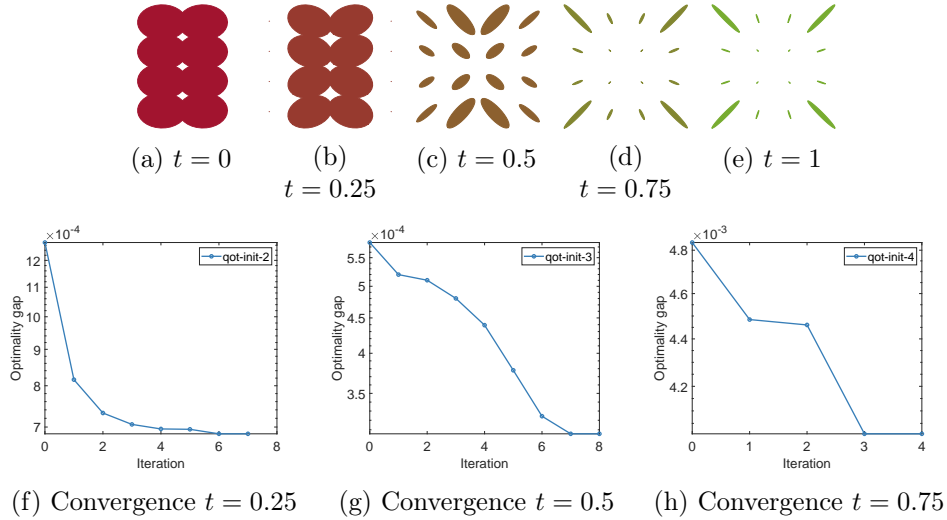


Figure 9: Tensor field Wasserstein barycenter ($n = 16$). The convergence for different barycenter is given in (f) to (h).

property, when $\mathbf{p} = \mathbf{q}$, we have $\mathbf{C}_{i,i} = \mathbf{0}$ and $\mathbf{C}_{i,j} \succ \mathbf{0}$ for $i \neq j$. Hence the optimal coupling would be a block diagonal matrix with $\mathbf{\Gamma}_{i,i} = p_i \mathbf{I}$. Hence $\text{MW}(\mathbf{p}, \mathbf{p}) = 0$. For the opposite direction, if $\text{MW}(\mathbf{p}, \mathbf{q}) = 0$, we always need to have $\mathbf{\Gamma}_{i,j} = \mathbf{0}$, for $i \neq j$ because $\text{tr}(\mathbf{C}_{i,j} \mathbf{\Gamma}_{i,j}) > 0$ for any $\mathbf{C}_{i,j} \succ \mathbf{0}$ and $i \neq j$. Thus we have $\mathbf{\Gamma}_{i,i} \neq \mathbf{0}$, which gives $\mathbf{C}_{i,i} = \mathbf{0}$ and $\mathbf{p} = \mathbf{q}$.

Finally, for triangle inequality, given $\mathbf{a}, \mathbf{b}, \mathbf{c} \in \Sigma_n$, and optimal matrix coupling $\mathbf{\Gamma}, \mathbf{\Delta}$ between (\mathbf{a}, \mathbf{b}) and (\mathbf{b}, \mathbf{c}) , respectively. That is, $\sum_j \mathbf{\Gamma}_{i,j} = a_i \mathbf{I}$, $\sum_i \mathbf{\Gamma}_{i,j} = b_j \mathbf{I}$ and similarly $\sum_j \mathbf{\Delta}_{i,j} = b_i \mathbf{I}$, $\sum_i \mathbf{\Delta}_{i,j} = c_j \mathbf{I}$. We now follow the same strategy by gluing the coupling $\mathbf{\Gamma}, \mathbf{\Delta}$ in [PC⁺19, Vil21]. That is, we define a coupling \mathbf{T} as

$$\mathbf{T}_{i,j} = \sum_k \frac{1}{2b_k} (\mathbf{\Gamma}_{i,k} \mathbf{\Delta}_{k,j} + \mathbf{\Delta}_{k,j} \mathbf{\Gamma}_{i,k}), \quad \forall i, j.$$

We can verify $\mathbf{T}_{i,j} \in \mathbb{S}_+^d$, given $\mathbf{\Gamma}_{i,j}, \mathbf{\Delta}_{i,j} \in \mathbb{S}_+^d$. Furthermore, we have $\forall i, j$,

$$\begin{aligned}\sum_j \mathbf{T}_{i,j} &= \sum_k \frac{1}{2b_k} (\mathbf{\Gamma}_{i,k} \sum_j \mathbf{\Delta}_{k,j} + \sum_j \mathbf{\Delta}_{k,j} \mathbf{\Gamma}_{i,k}) = \sum_k \mathbf{\Gamma}_{i,k} = a_i \mathbf{I}, \\ \sum_i \mathbf{T}_{i,j} &= \sum_k \frac{1}{2b_k} (\sum_i \mathbf{\Gamma}_{i,k} \mathbf{\Delta}_{k,j} + \mathbf{\Delta}_{k,j} \sum_i \mathbf{\Gamma}_{i,k}) = \sum_k \mathbf{\Delta}_{k,j} = c_j \mathbf{I}.\end{aligned}$$

Hence, $[\mathbf{T}_{i,j}]_{m \times n}$ is a valid coupling between (\mathbf{a}, \mathbf{c}) . Let $\mathbf{P}_i = a_i \mathbf{I}, \mathbf{Q}_j = c_j \mathbf{I}$ and the corresponding samples as $\mathbf{X}, \mathbf{Y}, \mathbf{Z}$ for measures $\mathbf{a}, \mathbf{b}, \mathbf{c}$ respectively. Then,

$$\begin{aligned}\text{MW}(\mathbf{a}, \mathbf{c}) &= \left(\min_{\mathbf{A} \in \Pi(n, n, d, \mathbf{P}, \mathbf{Q})} \sum_{i,j} \text{tr}(\mathbf{C}_{i,j} \mathbf{A}_{i,j}) \right)^{1/2} \leq \left(\sum_{i,j} \text{tr}(\mathbf{C}_{i,j} \mathbf{T}_{i,j}) \right)^{1/2} \\ &= \left(\sum_{i,j,k} \frac{1}{2b_k} \text{tr}(\mathbf{C}_{i,j} (\mathbf{\Gamma}_{i,k} \mathbf{\Delta}_{k,j} + \mathbf{\Delta}_{k,j} \mathbf{\Gamma}_{i,k})) \right)^{1/2} \\ &\leq \left(\sum_{i,j,k} \frac{1}{2b_k} \left(\sqrt{\text{tr}(\mathbf{C}_{i,k} (\mathbf{\Gamma}_{i,k} \mathbf{\Delta}_{k,j} + \mathbf{\Delta}_{k,j} \mathbf{\Gamma}_{i,k}))} + \sqrt{\text{tr}(\mathbf{C}_{k,j} (\mathbf{\Gamma}_{i,k} \mathbf{\Delta}_{k,j} + \mathbf{\Delta}_{k,j} \mathbf{\Gamma}_{i,k}))} \right)^2 \right)^{1/2} \\ &\leq \left(\sum_{i,j,k} \frac{1}{2b_k} \text{tr}(\mathbf{C}_{i,k} (\mathbf{\Gamma}_{i,k} \mathbf{\Delta}_{k,j} + \mathbf{\Delta}_{k,j} \mathbf{\Gamma}_{i,k})) \right)^{1/2} + \left(\sum_{i,j,k} \frac{1}{2b_k} \text{tr}(\mathbf{C}_{k,j} (\mathbf{\Gamma}_{i,k} \mathbf{\Delta}_{k,j} + \mathbf{\Delta}_{k,j} \mathbf{\Gamma}_{i,k})) \right)^{1/2} \\ &= \left(\sum_{i,k} \text{tr}(\mathbf{C}_{i,k} \mathbf{\Gamma}_{i,k}) \right)^{1/2} + \left(\sum_{k,j} \text{tr}(\mathbf{C}_{k,j} \mathbf{\Delta}_{k,j}) \right)^{1/2} \\ &= \text{MW}(\mathbf{a}, \mathbf{b}) + \text{MW}(\mathbf{b}, \mathbf{c}),\end{aligned}$$

where the second inequality is by assumption (iii) of the proposition and the third inequality is due to the Minkowski inequality. This completes the proof. \square

Proof of Proposition 4.3. Following [MS16], the projection is derived orthogonal with respect to the Riemannian metric (5) as

$$\mathbf{P}_{\mathbf{\Gamma}}(\mathbf{S}) = \arg \min_{\mathbf{U} \in T_{\mathbf{\Gamma}} \mathcal{M}_{m,n}^d} f(\mathbf{U}) = -g_{\mathbf{\Gamma}}(\mathbf{U}, \mathbf{S}) + \frac{1}{2} g_{\mathbf{\Gamma}}(\mathbf{U}, \mathbf{U}). \quad (11)$$

The Lagrangian of problem (11) is

$$f(\mathbf{U}) - \text{tr}(\mathbf{\Lambda}_i \sum_j \mathbf{U}_{i,j}) - \text{tr}(\mathbf{\Theta}_j \sum_i \mathbf{U}_{i,j}), \quad (12)$$

where $\mathbf{\Lambda}_i, \mathbf{\Theta}_j$ are dual variables for $i \in [m], j \in [n]$. The orthogonal projection follows from the stationary conditions of (12). \square

Proof of Proposition 4.4. Given the manifold $\mathcal{M}_{m,n}^d$ is a submanifold of $\times_{m,n} \mathbb{S}_{++}^d$ with affine-invariant (AI) Riemannian metric, the Riemannian gradient is given by

$$\text{grad}F(\mathbf{\Gamma}) = \mathbf{P}_{\mathbf{\Gamma}}([\text{grad}_{\text{ai}}F(\mathbf{\Gamma}_{i,j})]_{m \times n}) = \mathbf{P}_{\mathbf{\Gamma}}([\mathbf{\Gamma}_{i,j} \{ \nabla F(\mathbf{\Gamma}_{i,j}) \} \mathbf{\Gamma}_{i,j}]_{m \times n}),$$

where $\text{grad}_{\text{ai}}F(\mathbf{X})$ is the Riemannian gradient of $\mathbf{X} \in \mathbb{S}_{++}^d$ with AI metric. Similarly, the Riemannian Hessian $\text{Hess}F(\mathbf{\Gamma})[\mathbf{U}] = \nabla_{\mathbf{U}}\text{grad}F(\mathbf{\Gamma})$ where here ∇ denotes the covariant derivative (i.e., Riemannian connection). For submanifold, the connection $\nabla_{\mathbf{U}}\text{grad}F(\mathbf{\Gamma}) = \text{P}_{\mathbf{\Gamma}}([\tilde{\nabla}_{\mathbf{U}_{i,j}}(\text{grad}F(\mathbf{\Gamma}_{i,j}))]_{m \times n})$ where $\tilde{\nabla}$ represents the connection of \mathbb{S}_{++}^d . According to [Bha09], $\tilde{\nabla}_{\mathbf{U}_{i,j}}\text{grad}F(\mathbf{\Gamma}_{i,j}) = \text{Dgrad}F(\mathbf{\Gamma}_{i,j})[\mathbf{U}_{i,j}] - \{\mathbf{U}_{i,j}\mathbf{\Gamma}_{i,j}^{-1}\text{grad}F(\mathbf{\Gamma}_{i,j})\}_{\text{S}}$. Hence, the proof is complete. \square

Proof of Theorem 4.5. We first write the Lagrange dual function as

$$g(\mathbf{\Lambda}, \mathbf{\Theta}, \mathbf{\Psi}) = \min_{\mathbf{\Gamma}=[\mathbf{\Gamma}_{i,j}]_{m \times n}} F(\mathbf{\Gamma}) + \sum_i \text{tr}\left(\mathbf{\Lambda}_i\left(\sum_j \mathbf{\Gamma}_{i,j} - \mathbf{P}_i\right)\right) + \sum_j \text{tr}\left(\mathbf{\Theta}_j\left(\sum_i \mathbf{\Gamma}_{i,j} - \mathbf{Q}_j\right)\right) - \sum_{i,j} \text{tr}\left(\mathbf{\Psi}_{i,j}\mathbf{\Gamma}_{i,j}\right),$$

where we relax the SPD constraint on $\mathbf{\Gamma}_{i,j}$ to the semidefinite constraint, i.e. $\mathbf{\Gamma}_{i,j} \succeq \mathbf{0}$, for some dual variable $\mathbf{\Lambda}_i, \mathbf{\Theta}_j \in \mathbb{S}^d$ and $\mathbf{\Psi}_{i,j} \succeq \mathbf{0}$. Given the function F is convex with non-empty constraint set, by Slater's condition, strong duality holds and the primal and dual variables should jointly satisfy the KKT conditions.

First, we notice by complementary slackness, $\text{tr}(\mathbf{\Psi}_{i,j}^*\mathbf{\Gamma}_{i,j}^*) = 0$ for $\mathbf{\Gamma}_{i,j}^* \succ \mathbf{0}$. This implies that $\mathbf{\Psi}_{i,j}^* = \mathbf{0}$ since $\mathbf{\Psi}_{i,j}^* \succeq \mathbf{0}$. Note that in some cases $\mathbf{\Gamma}_{i,j}^*$ may be rank-deficient (i.e., some eigenvalues are close to zero), which gives rise to non-zero $\mathbf{\Psi}_{i,j}^*$. Regardless, from the optimality condition, it always satisfies for optimal $\mathbf{\Gamma}_{i,j}^*, \mathbf{\Lambda}_i^*, \mathbf{\Theta}_j^*$,

$$\mathbf{\Gamma}_{i,j}^*(\nabla F(\mathbf{\Gamma}_{i,j}^*) + \mathbf{\Lambda}_i^* + \mathbf{\Theta}_j^*)\mathbf{\Gamma}_{i,j}^* = \mathbf{0}, \quad (13)$$

due to that $\mathbf{\Gamma}_{i,j}^*$ is orthogonal to $\mathbf{\Psi}_{i,j}^*$. $\nabla F(\mathbf{\Gamma}_{i,j}^*)$ denotes the block partial derivative of F with respect to $\mathbf{\Gamma}_{i,j}$ at optimality.

On the other hand, to perform Riemannian optimization, the Riemannian gradient is first computed for the primal objective F as

$$\text{grad}F(\mathbf{\Gamma}) = \text{P}_{\mathbf{\Gamma}}([\mathbf{\Gamma}_{i,j}\{\nabla F(\mathbf{\Gamma}_{i,j})\}_{\text{S}}\mathbf{\Gamma}_{i,j}]_{m \times n}),$$

which from the definition of orthogonal projection, gives

$$\text{grad}F(\mathbf{\Gamma}_{i,j}) = \mathbf{\Gamma}_{i,j}\left(\nabla F(\mathbf{\Gamma}_{i,j}) + \tilde{\mathbf{\Lambda}}_i + \tilde{\mathbf{\Theta}}_j\right)\mathbf{\Gamma}_{i,j},$$

where $\text{grad}F(\mathbf{\Gamma}_{i,j})$ represents the Riemannian partial derivative and $\tilde{\mathbf{\Lambda}}_i, \tilde{\mathbf{\Theta}}_j \in \mathbb{S}^d$ are computed such that

$$\begin{cases} \sum_i \mathbf{\Gamma}_{i,j}(\mathbf{C}_{i,j} + \epsilon \nabla \Omega(\mathbf{\Gamma}_{i,j}^*) + \tilde{\mathbf{\Lambda}}_i + \tilde{\mathbf{\Theta}}_j)\mathbf{\Gamma}_{i,j} = \mathbf{0}, & \forall j \\ \sum_j \mathbf{\Gamma}_{i,j}(\mathbf{C}_{i,j} + \epsilon \nabla \Omega(\mathbf{\Gamma}_{i,j}^*) + \tilde{\mathbf{\Lambda}}_i + \tilde{\mathbf{\Theta}}_j)\mathbf{\Gamma}_{i,j} = \mathbf{0}, & \forall i. \end{cases} \quad (14)$$

Comparing (14) to (13), we see that at optimality, there exists $\mathbf{\Lambda}_i^*, \mathbf{\Theta}_j^*$ such that for all i, j , the conditions (14) are satisfied, with $\tilde{\mathbf{\Lambda}}_i = \mathbf{\Lambda}_i^* + \Delta$, $\tilde{\mathbf{\Theta}}_j = \mathbf{\Theta}_j^* - \Delta$, for any symmetric matrix Δ . Hence, the Riemannian gradient at optimality $\text{grad}F(\mathbf{\Gamma}_{i,j}^*) = \mathbf{0}$, thus completing the proof. \square

Proof of Proposition 5.1. For each regularized OT problem, we consider the Lagrange dual problem of $\min_{\Gamma \in \mathcal{M}_{m,n}^d} \text{MW}_\epsilon(\bar{\mathbf{P}}, \mathbf{P}^\ell)$, which is given as

$$\mathcal{L}_{\text{MW}_\epsilon} = \max_{\substack{\Lambda_i^\ell, \Theta_j^\ell \in \mathbb{S}^d \\ \Psi_{i,j}^\ell \succeq \mathbf{0}}} \left(\min_{\Gamma_{i,j}^\ell} \sum_{i,j} (\text{tr}(\mathbf{C}_{i,j}^\ell \Gamma_{i,j}^\ell) + \epsilon \Omega(\Gamma_{i,j}^\ell)) \right) \quad (15)$$

$$+ \sum_i \text{tr}(\Lambda_i^\ell (\sum_j \Gamma_{i,j}^\ell - \bar{\mathbf{P}}_i)) + \sum_j \text{tr}(\Theta_j^\ell (\sum_i \Gamma_{i,j}^\ell - \mathbf{P}_j^\ell)) - \sum_{i,j} \text{tr}(\Psi_{i,j}^\ell \Gamma_{i,j}^\ell). \quad (16)$$

From the Lagrangian (16), it is easy to see the Euclidean gradient of the barycenter problem with respect to $\bar{\mathbf{P}}_i$ is $-\sum_\ell \Lambda_i^\ell$ with the dual optimal Λ_i^ℓ for problem (16). Next, the proof is complete by substituting the objective $F(\Gamma) = \sum_{i,j} (\text{tr}(\mathbf{C}_{i,j}^\ell \Gamma_{i,j}^\ell) + \epsilon \Omega(\Gamma_{i,j}^\ell))$ as in Theorem 4.5. \square

Proof of Proposition 5.2. First we rewrite SPD matrix-valued GW discrepancy as

$$\begin{aligned} \text{MGW}((\bar{\mathbf{D}}, \bar{\mathbf{P}}), (\mathbf{D}^\ell, \mathbf{P}^\ell)) &= \sum_{i,i',j,j'} \left(f_1(\bar{D}_{i,i'}) + f_2(D_{j,j'}^\ell) - h_1(\bar{D}_{i,i'}) h_2(D_{j,j'}^\ell) \right) \text{tr}(\Gamma_{i,j}^\ell \Gamma_{i',j'}^\ell) \\ &= \sum_{i,j} \text{tr} \left(\Gamma_{i,j} \left(\sum_{i'} f_1(\bar{D}_{i,i'}) \bar{\mathbf{P}}_{i'} + \sum_{j'} f_2(D_{j,j'}^\ell) \mathbf{P}_{j'}^\ell - \sum_{i'} h_1(\bar{D}_{i,i'}) \sum_{j'} h_2(D_{j,j'}^\ell) \Gamma_{i',j'}^\ell \right) \right), \end{aligned}$$

where we use the fact that $\Gamma_{i,j}^\ell$ are optimal and satisfy the constraints $\sum_j \Gamma_{i,j}^\ell = \bar{\mathbf{P}}_i$ and $\sum_i \Gamma_{i,j}^\ell = \mathbf{P}_j^\ell$. By the first order condition, we have

$$\text{tr} \left(\bar{\mathbf{P}}_i f_1'(\bar{D}_{i,i'}) \bar{\mathbf{P}}_{i'} - h_1'(\bar{D}_{i,i'}) \sum_j \Gamma_{i,j} \left(\sum_{j'} h_2(D_{j,j'}^\ell) \Gamma_{i',j'}^\ell \right) \right) = 0, \quad \forall i, i' \in [m],$$

which gives the desired result. \square

E Projection and MW (2) for probability measures

For given marginals $\mathbf{p} \in \Sigma_m$ and $\mathbf{q} \in \Sigma_n$, i.e., $\sum_i p_i = \sum_j q_j = 1$, for $p_i, q_j \geq 0$, we consider the corresponding block SPD marginals \mathbf{P} and \mathbf{Q} be defined as $\mathbf{P} := \{[\mathbf{P}_i]_{m \times 1} : \mathbf{P}_i = p_i \mathbf{I}\}$ and $\mathbf{Q} := \{[\mathbf{Q}_j]_{n \times 1} : \mathbf{Q}_j = q_j \mathbf{I}\}$ in the $d \times d$ space and so are the cost matrices $[\mathbf{C}_{i,j}]_{m \times n}$.

For this case, we introduce a projected variant of the SPD matrix-valued optimal transport problem by parameterizing the coupling block-matrix $[\Gamma_{i,j}]_{m \times n}$ as $\Gamma_{i,j} = \mathbf{W} \Gamma_{i,j}^r \mathbf{W}^\top$, where $\Gamma_{i,j}^r \succeq \mathbf{0}$ is of size $r \times r$ and $\mathbf{W} \in \mathbb{R}^{d \times r}$. Imposing the projection constraint that $\mathbf{W}^\top \mathbf{W} = \mathbf{I}^r$ ($r \times r$ identity matrix), we observe the new block-SPD marginals $[\Gamma_{i,j}^r]_{m \times n}$ become consistent for the probability measures \mathbf{p} and \mathbf{q} . Equivalently, $\mathbf{P}^r := \{[\mathbf{P}_i^r]_{m \times 1} : \mathbf{P}_i^r = p_i \mathbf{I}^r\}$ and $\mathbf{Q}^r := \{[\mathbf{Q}_j^r]_{n \times 1} : \mathbf{Q}_j^r = q_j \mathbf{I}^r\}$. In other words, both \mathbf{P} and \mathbf{P}^r can be considered as the lifting of \mathbf{p} but onto different spaces. Similarly for \mathbf{Q} and \mathbf{Q}^r . In particular, the cost $\mathbf{C}_{i,j}^r$ is related to $\mathbf{C}_{i,j}$ as $\mathbf{C}_{i,j}^r = \mathbf{W}^\top \mathbf{C}_{i,j} \mathbf{W}$. This motivates to consider the formulation

$$\min_{\mathbf{W}^\top \mathbf{W} = \mathbf{I}^r} / \max_{\mathbf{W}^\top \mathbf{W} = \mathbf{I}^r} \sum_{i,j} \min_{\Gamma_{i,j}^r \in \Pi(m,n,r, \mathbf{P}^r, \mathbf{Q}^r)} \text{MW}^2(\mathbf{p}, \mathbf{q}; \mathbf{W}) := \text{tr}(\mathbf{C}_{i,j} \mathbf{W} \Gamma_{i,j}^r \mathbf{W}^\top) = \text{tr}(\mathbf{W}^\top \mathbf{C}_{i,j} \mathbf{W} \Gamma_{i,j}^r), \quad (17)$$

which aims to simultaneously optimize the coupling as well as a projection $\mathbf{W} \in \mathbb{R}^{d \times r}$. For learning the optimal projection \mathbf{W} in (17), both minimization and maximization make sense depending on applications.

Let us define the projection robust MW OT problem as

$$\text{PRMW}_r^2(\mathbf{p}, \mathbf{q}) = \max_{\mathbf{W}^\top \mathbf{W} = \mathbf{I}^r} \sum_{i,j} \min_{\Gamma^r \in \Pi(m,n,r, \mathbf{P}^r, \mathbf{Q}^r)} \text{MW}^2(\mathbf{p}, \mathbf{q}; \mathbf{W}). \quad (18)$$

Proposition E.1. *Suppose the marginals $\mathbf{p}, \mathbf{q} \in \Sigma_n$ have the same support, the cost matrices $[\mathbf{C}_{i,j}]_{m \times n}$ satisfy the properties in Proposition 3.1, and $\text{MW}(\mathbf{p}, \mathbf{q})$ is a metric between the marginals \mathbf{p} and \mathbf{q} . Then, $\text{PRMW}(\mathbf{p}, \mathbf{q})$ is also a metric between the marginals \mathbf{p} and \mathbf{q} .*

Proof. As the cost matrices $[\mathbf{C}_{i,j}]_{m \times n}$ satisfy the properties in Proposition 3.1, it is easy to see that the cost matrices $[\mathbf{C}_{i,j}^r]_{m \times n}$ satisfy the properties as well. Consequently, $\text{MW}(\mathbf{p}, \mathbf{q}; \mathbf{W})$ is a metric for a given projection matrix \mathbf{W} .

It is straightforward to see that $\text{PRMW}_r(\mathbf{p}, \mathbf{q}) = \text{PRMW}_r(\mathbf{q}, \mathbf{p})$ and $\text{PRMW}_r(\mathbf{p}, \mathbf{q}) = 0$ if and only if $\mathbf{p} = \mathbf{q}$. The remaining property of triangle inequality for $\text{PRMW}_r(\mathbf{p}, \mathbf{q})$ follows as shown below. Let

$$\mathbf{W}^* = \arg \max_{\mathbf{W}^\top \mathbf{W} = \mathbf{I}^r} \sum_{i,j} \min_{\Gamma^r \in \Pi(m,n,r, \mathbf{P}^r, \mathbf{Q}^r)} \text{MW}^2(\mathbf{p}, \mathbf{q}; \mathbf{W}). \quad (19)$$

Therefore, from (19), we have

$$\begin{aligned} \text{PRMW}_r(\mathbf{p}, \mathbf{q}) &= \text{MW}(\mathbf{p}, \mathbf{q}; \mathbf{W}^*) \\ &\leq \text{MW}(\mathbf{p}, \tilde{\mathbf{q}}; \mathbf{W}^*) + \text{MW}(\tilde{\mathbf{q}}, \mathbf{q}; \mathbf{W}^*) \text{ as MW is a metric} \\ &\leq \text{PRMW}_r(\mathbf{p}, \tilde{\mathbf{q}}) + \text{PRMW}_r(\tilde{\mathbf{q}}, \mathbf{q}). \end{aligned}$$

This completes the proof. \square

F Trace-constrained block SPD coupling manifold

Given the set $\mathcal{M}_{m,n}^d$ might be empty for general block-SPD marginals, here we consider a relaxation of the coupling constraint, where only the sum of traces of the row and columns blocks need to be matched with the trace of block-SPD marginals [PCVS19, NGT14]. That is,

$$\tilde{\mathcal{M}}_{m,n}^d(\mathbf{p}, \mathbf{q}) := \{\Gamma : \Gamma_{i,j} \in \mathbb{S}_{++}^d, \sum_j \text{tr}(\Gamma_{i,j}) = p_i, \sum_i \text{tr}(\Gamma_{i,j}) = q_j\},$$

where $\sum_i p_i = \sum_j q_j = 1$. We show such set can also be endowed with a manifold structure, thus facilitating optimization with such constraint.

The tangent space characterization of $\tilde{\mathcal{M}}_{m,n}^d$ at Γ is given by

$$\begin{aligned} T_\Gamma \tilde{\mathcal{M}}_{m,n}^d &= \{[\mathbf{U}_{i,j}]_{m \times n} : \mathbf{U}_{i,j} \in \mathbb{S}^d, \\ &\quad \sum_i \text{tr}(\mathbf{U}_{i,j}) = 0, \sum_j \text{tr}(\mathbf{U}_{i,j}) = 0\}. \end{aligned}$$

With the same Riemannian metric in (5), the orthogonal projection (Proposition 4.3) can be simplified as

$$\tilde{\mathbf{P}}_\Gamma(\mathbf{S}) = \mathbf{U}, \text{ with } \mathbf{U}_{i,j} = \mathbf{S}_{i,j} + (\lambda_i + \theta_j) \Gamma_{i,j}^2, \quad (20)$$

where λ_i, θ_j can be computed from

$$\begin{cases} -\sum_i \text{tr}(\mathbf{S}_{i,j}) = \sum_i (\lambda_i + \theta_j) \text{tr}(\mathbf{\Gamma}_{i,j}^2), & \forall j, \\ -\sum_j \text{tr}(\mathbf{S}_{i,j}) = \sum_j (\lambda_i + \theta_j) \text{tr}(\mathbf{\Gamma}_{i,j}^2), & \forall i. \end{cases}$$

The Riemannian gradient and Hessian exactly follows from Proposition 4.4 with projection replaced by (20).

Retraction and trace-constrained block matrix balancing algorithm. Although we can follow the same iterative strategy of normalizing the rows and columns as in Algorithm 2, one naïve and efficient alternative is to simply solve a classic scalar OT problem for the trace of each block.

Denote $\tilde{a}_{i,j} = \text{tr}(\mathbf{A}_{i,j})$ and consider a matrix $\tilde{\mathbf{A}} = [\tilde{a}_{i,j}]_{m \times n}$, with $\tilde{a}_{i,j} > 0$. We can perform the scalar Sinkhorn algorithm with marginals \mathbf{p} and \mathbf{q} , which gives a balanced matrix $\tilde{\mathbf{B}}$ that satisfies $\tilde{\mathbf{B}}\mathbf{1} = \mathbf{p}$ and $\tilde{\mathbf{B}}^\top \mathbf{1} = \mathbf{q}$. Denote its entries as $\tilde{b}_{i,j}$. Then the block matrix that satisfies the trace coupling constraints is given by $[\mathbf{B}_{i,j}]_{m \times n}$ with $\mathbf{B}_{i,j} = \frac{\tilde{b}_{i,j}}{\tilde{a}_{i,j}} \mathbf{A}_{i,j}$ because we see $\sum_i \text{tr}(\mathbf{B}_{i,j}) = \sum_i \tilde{b}_{i,j} = \nu_j, \forall j$ and $\sum_j \text{tr}(\mathbf{B}_{i,j}) = \mu_i$. We notice that there are many other approaches to perform diagonal scaling such that the trace coupling constraints are satisfied. See Section F.1 for more details.

Similar to (6), the retraction is given by

$$R_{\mathbf{\Gamma}}(\mathbf{U}) = \text{trBalance}([\mathbf{\Gamma}_{i,j} \exp(\mathbf{\Gamma}_{i,j}^{-1} \mathbf{U}_{i,j})]_{m \times n}),$$

where trBalance denotes the process of balancing the trace of matrix to satisfy the coupling constraints. To verify this is indeed a retraction, we follow the same strategy as in [DH19, SGH⁺21]. This is formalized in Proposition F.1.

Proposition F.1. *The operation $R_{\mathbf{\Gamma}}(\mathbf{U}) = \text{trBalance}([\mathbf{\Gamma}_{i,j} \exp(\mathbf{\Gamma}_{i,j}^{-1} \mathbf{U}_{i,j})]_{m \times n})$ is a valid retraction for the manifold $\tilde{\mathcal{M}}_{m,n}^d$.*

Proof. The first condition of retraction is clearly satisfied. For the second condition, Sinkhorn's Theorem shows that for any positive matrix $\tilde{\mathbf{A}}$, it can be scaled to a unique coupling matrix of the form $\tilde{\mathbf{B}} = \mathbf{D}_1 \tilde{\mathbf{A}} \mathbf{D}_2$, where the diagonal matrices $\mathbf{D}_1, \mathbf{D}_2$ are unique up to scaling [Sin64]. Suppose the scaling is given by $\alpha_i \beta_j \tilde{\mathbf{A}}_{i,j}$ with $\alpha_i, \beta_j > 0, \forall i, j$. Then we can easily verify that $\alpha_i \beta_j = \tilde{b}_{i,j} / \tilde{a}_{i,j}$ are unique. This simply follows from the uniqueness of the scaling factors for $\tilde{\mathbf{A}}$.

Given $[\mathbf{\Gamma}_{i,j}] \in \tilde{\mathcal{M}}_{m,n}^d$ and also $[\alpha_i \beta_j \mathbf{\Gamma}_{i,j}] \in \tilde{\mathcal{M}}_{m,n}^d$, we see $\alpha_i = \beta_j = 1$ by uniqueness. From the constraint $\sum_i \text{tr}(\alpha_i \beta_j \mathbf{\Gamma}_{i,j}) = \nu_j, \sum_j \text{tr}(\alpha_i \beta_j \mathbf{\Gamma}_{i,j}) = \mu_i$, we take differential of both sides, which gives

$$\sum_i \text{tr}(\partial \alpha_i \mathbf{\Gamma}_{i,j} + \partial \beta_j \mathbf{\Gamma}_{i,j}) = \sum_j \text{tr}(\partial \alpha_i \mathbf{\Gamma}_{i,j} + \partial \beta_j \mathbf{\Gamma}_{i,j}) = 0.$$

Using similar argument, we can verify $\partial \alpha_i = -\gamma \partial \beta_j$ and thus it gives $\text{trBalance}(\mathbf{\Gamma} + \partial \mathbf{\Gamma}) \approx \mathbf{\Gamma} + \partial \mathbf{\Gamma}$. This further leads to $DR_{\mathbf{\Gamma}}(\mathbf{0})[\mathbf{U}] = \mathbf{U}$. \square

F.1 Alternative balancing approaches for trace coupling constraint

Alternatively, we may consider a matrix log-barrier formulation as follows. Let $\mathbf{c}_j \in \mathbb{R}_{++}^d, j \in [m]$ and $\mathbf{r}_i \in \mathbb{R}_{++}^d, i \in [n]$ be two sets of positive scaling factors. We consider the following optimization

problem:

$$\begin{aligned} \min g(\mathbf{c}_{1:m}, \mathbf{r}_{1:n}) := & \sum_{i,j} \text{tr}(\text{diag}(\mathbf{c}_j) \text{diag}(\mathbf{r}_i) \mathbf{A}_{i,j} \text{diag}(\mathbf{r}_i) \text{diag}(\mathbf{c}_j)) \\ & - \frac{2}{d} \sum_i \mu_i \log \det(\text{diag}(\mathbf{r}_i)) - \frac{2}{d} \sum_j \nu_j \log \det(\text{diag}(\mathbf{c}_j)) \end{aligned} \quad (21)$$

This problem is clearly convex for each argument given the other fixed. Hence, one strategy is block coordinate descent. The first order conditions are given by

$$\frac{\partial g}{\partial \mathbf{c}_j} = 2 \sum_i (\mathbf{r}_i)^2 \odot \text{diag}(\mathbf{A}_{i,j}) \odot \mathbf{c}_j - \frac{2\nu_j}{d} \mathbf{c}_j^{-1} = \mathbf{0}, \quad \forall j \quad (22)$$

$$\frac{\partial g}{\partial \mathbf{r}_i} = 2 \sum_j (\mathbf{c}_j)^2 \odot \text{diag}(\mathbf{A}_{i,j}) \odot \mathbf{r}_i - \frac{2\mu_i}{d} \mathbf{r}_i^{-1} = \mathbf{0}, \quad \forall i, \quad (23)$$

where the \odot and the square stand for elementwise product and elementwise square. diag represents the diagonal operation as either extracting the diagonal elements or forming a diagonal matrix depending on the input. $\mathbf{1}$ denotes the vector of all ones.

This gives an alternating strategy to update the variables similar to the classic Sinkhorn-Knopp algorithm

$$\begin{aligned} \mathbf{c}_j & \leftarrow \left(\nu_j \mathbf{1} / (d \sum_i (\mathbf{r}_i)^2 \odot \text{diag}(\mathbf{A}_{i,j})) \right)^{1/2}, \quad \forall j \\ \mathbf{r}_i & \leftarrow \left(\mu_i \mathbf{1} / (d \sum_j (\mathbf{c}_j)^2 \odot \text{diag}(\mathbf{A}_{i,j})) \right)^{1/2}, \quad \forall i. \end{aligned} \quad (24)$$

We notice that any stationary points $\mathbf{r}_i^*, \mathbf{c}_j^*, \forall i, j$ satisfying (22), (23) scale the block SPD matrices to satisfy the row and column trace constrained. This is because

$$\begin{aligned} \sum_i \text{tr}(\text{diag}(\mathbf{c}_j^*) \text{diag}(\mathbf{r}_i^*) \mathbf{A}_{i,j} \text{diag}(\mathbf{r}_i^*) \text{diag}(\mathbf{c}_j^*)) &= \sum_i ((\mathbf{c}_j^*)^2 \odot (\mathbf{r}_i^*)^2 \odot \text{diag}(\mathbf{A}_{i,j}))^\top \mathbf{1} \\ &= \sum_i (\nu_j / d \mathbf{1})^\top \mathbf{1} = \nu_j. \end{aligned}$$

The similar result holds for row sum. Hence, for any block SPD matrix \mathbf{A} , it can be scaled to satisfy the row and column trace sum constrained if and only if the optimization (21) has a stationary point. From here, many existing results concerning existence and uniqueness as well as convergence are readily applied because the iterative update in (24) is a multivariate version of classic Sinkhorn-Knopp update applied elementwise. See for example [Kni08].

G Riemannian geometry for block SPD Wasserstein barycenter

Riemannian geometry of $\Delta_n(\mathbb{S}_{++}^d)$. In [MKJ19], the authors endow a Riemannian manifold structure for the set $\Delta_n(\mathbb{S}_{++}^d) := \{\mathbf{P} = [\mathbf{P}_i]_{n \times 1} : \sum_i \mathbf{P}_i = \mathbf{I}\}$. The manifold is defined as

$$\Delta_n(\mathbb{S}_{++}^d) := \{(\mathbf{P}_1, \mathbf{P}_2, \dots, \mathbf{P}_n) : \mathbf{P}_i \in \mathbb{S}_{++}^d, \sum_i \mathbf{P}_i = \mathbf{I}\}.$$

Its tangent space is given by

$$T_{\mathbf{P}}\Delta_n(\mathbb{S}_{++}^d) = \{(\mathbf{U}_1, \dots, \mathbf{U}_n) : \mathbf{U}_i \in \mathbb{S}^d, \sum_i \mathbf{U}_i = \mathbf{0}\}.$$

By introducing a similar affine-invariant metric $\langle \mathbf{U}, \mathbf{V} \rangle_{\mathbf{P}} = \sum_i \text{tr}(\mathbf{P}_i^{-1} \mathbf{U}_i \mathbf{P}_i^{-1} \mathbf{V}_i)$. The retraction from the tangent space to manifold is derived as

$$R_{\mathbf{P}}(\mathbf{U}) = (\hat{\mathbf{P}}_{\text{sum}}^{-1/2} \hat{\mathbf{P}}_1 \hat{\mathbf{P}}_{\text{sum}}^{-1/2}, \dots, \hat{\mathbf{P}}_{\text{sum}}^{-1/2} \hat{\mathbf{P}}_n \hat{\mathbf{P}}_{\text{sum}}^{-1/2}),$$

where $\hat{\mathbf{P}}_i = \mathbf{P}_i(\exp(\mathbf{P}_i^{-1} \mathbf{U}_i))$ and $\hat{\mathbf{P}}_{\text{sum}} = \sum_i \hat{\mathbf{P}}_i$.

The Riemannian gradient of a function $F : \Delta_n(\mathbb{S}_{++}^d) \rightarrow \mathbb{R}$ is computed as

$$\text{grad}F(\mathbf{P}) = P_{\mathbf{P}}\left(\left(\mathbf{P}_1\{\nabla F(\mathbf{P}_1)\}_{\mathbf{S}\mathbf{P}_1}, \dots, \mathbf{P}_n\{\nabla F(\mathbf{P}_n)\}_{\mathbf{S}\mathbf{P}_n}\right)\right),$$

where the orthogonal projection $P_{\mathbf{P}}$ of a of $\mathbf{S} = (\mathbf{S}_1, \mathbf{S}_2, \dots, \mathbf{S}_n)$ such that $\mathbf{S}_i \in \mathbb{S}^d$ is

$$P_{\mathbf{X}}(\mathbf{S}) = (\mathbf{S}_1 + \mathbf{P}_1 \mathbf{\Lambda} \mathbf{P}_1, \dots, \mathbf{S}_n + \mathbf{P}_n \mathbf{\Lambda} \mathbf{P}_n),$$

where $\mathbf{\Lambda} \in \mathbb{S}^d$ is the solution to the linear equation $\sum_i \mathbf{P}_i \mathbf{\Lambda} \mathbf{P}_i = -\sum_i \mathbf{S}_i$.

Optimization for Wasserstein barycenter. With the Riemannian geometry defined for the simplex of SPD matrices, we can update the barycenter by Riemannian optimization as shown in Algorithm 3.

Algorithm 3 Block-SPD Wasserstein barycenter

- 1: **Input:** block-SPD marginals $\{\mathbf{P}^\ell\}_{\ell=1}^K$, cost matrices $\{\mathbf{C}^\ell\}_{\ell=1}^K$.
 - 2: Initialize $\bar{\mathbf{P}}^0$ as uniform distribution.
 - 3: **for** $t = 1, \dots, T$ **do**
 - 4: **for** $\ell = 1, \dots, K$ **do**
 - 5: Compute $(\mathbf{\Lambda}^\ell)^*$ as in Proposition 5.1.
 - 6: **end for**
 - 7: Compute the Riemannian gradient of (7) by orthogonally projecting $\sum_\ell \omega_\ell (\mathbf{\Lambda}^\ell)^*$ onto the tangent space of $\Delta_n(\mathbb{S}_{++}^d)$.
 - 8: Update $\bar{\mathbf{P}}^t$ by retracting on $\Delta_n(\mathbb{S}_{++}^d)$ with a step size.
 - 9: **end for**
 - 10: **Output:** Barycenter $\bar{\mathbf{P}}^T$.
-